

Ultrafast Materials Physics

Ian Robinson
Jesse Clark
Ross Harder
Gang Xiong
Marcus Newton
Felix Hofmann

Brookhaven National Laboratory
London Centre for Nanotechnology

Physics Colloquium,
Arizona State University
Tempe, April 2018

Outline

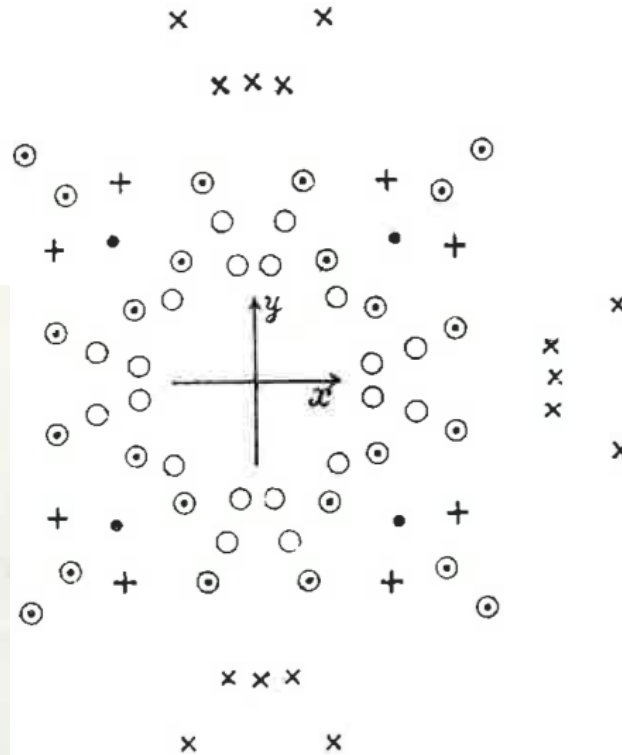
- Bragg Coherent Diffraction Imaging
- Nanocrystal structures
- Crystal strain as complex density
- Nanoscale alloying
- Ultrafast snapshots of moving matter
- Strain Tensor imaging

Max von Laue, 1879-1960

Proceedings Bavarian Academy of Sciences, 1912

Zinc Blende, ZnS, Nobel prize 1914

- $\lambda/\alpha = 0,0377$
- ⊙ $\lambda/\alpha = 0,0563$
- × $\lambda/\alpha = 0,0663$
- $\lambda/\alpha = 0,1051$
- + $\lambda/\alpha = 0,143$



W. L. Bragg 1890-1971

THE DIFFRACTION OF SHORT ELECTROMAGNETIC WAVES BY A CRYSTAL

by

W. L. Bragg, B. A., Trinity College

(communicated by Prof. Sir J. J. Thomson)

(Read 11 November 1912)

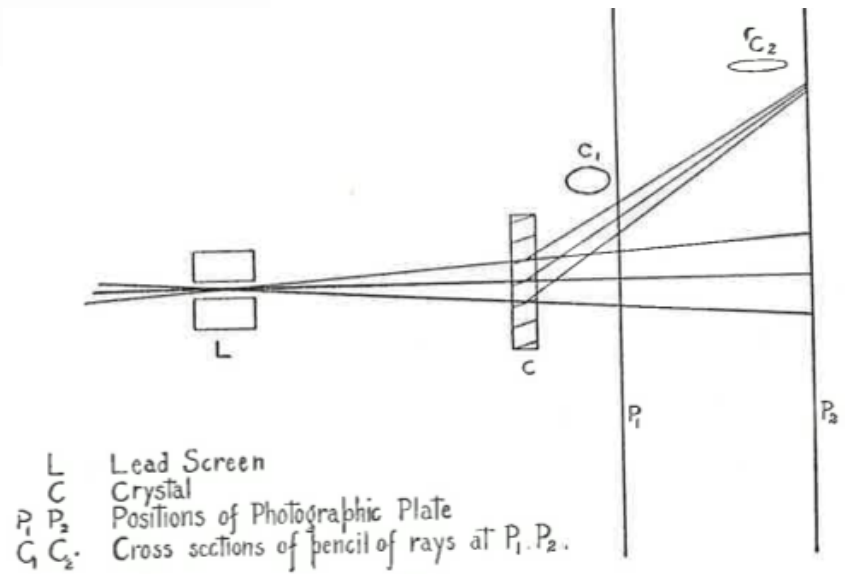
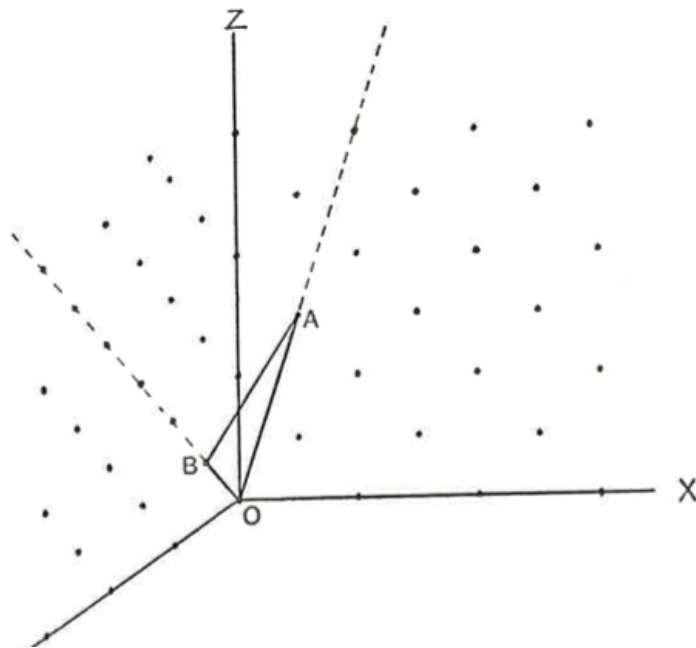
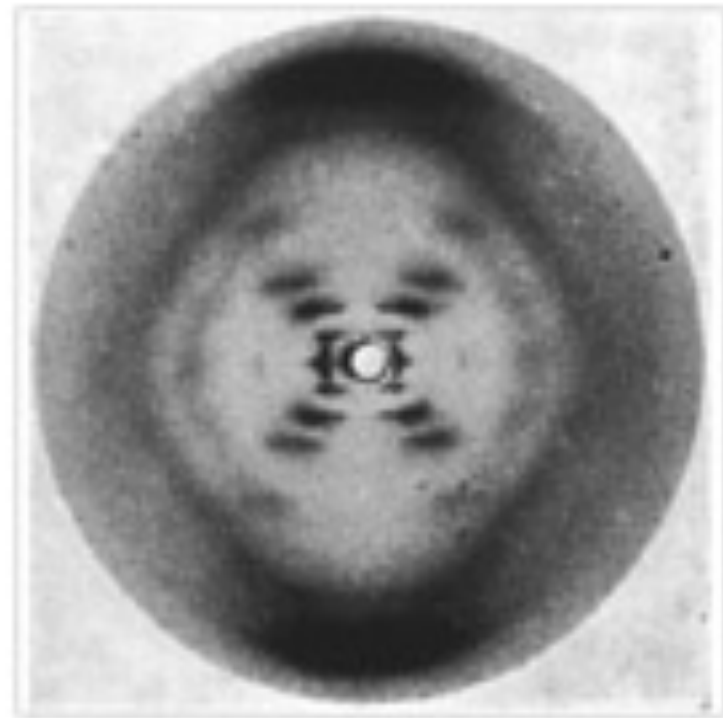


Fig. 2.

Diffraction as Fourier Transform

Rosalind Franklin's DNA "photo 51" 1952

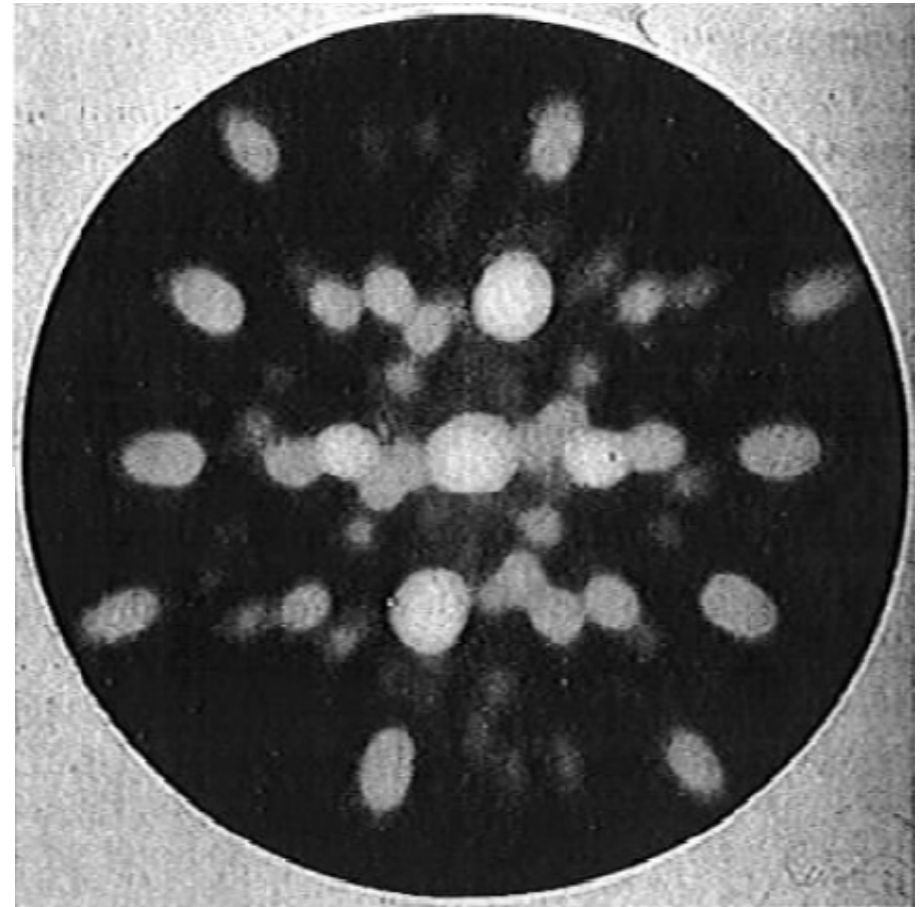
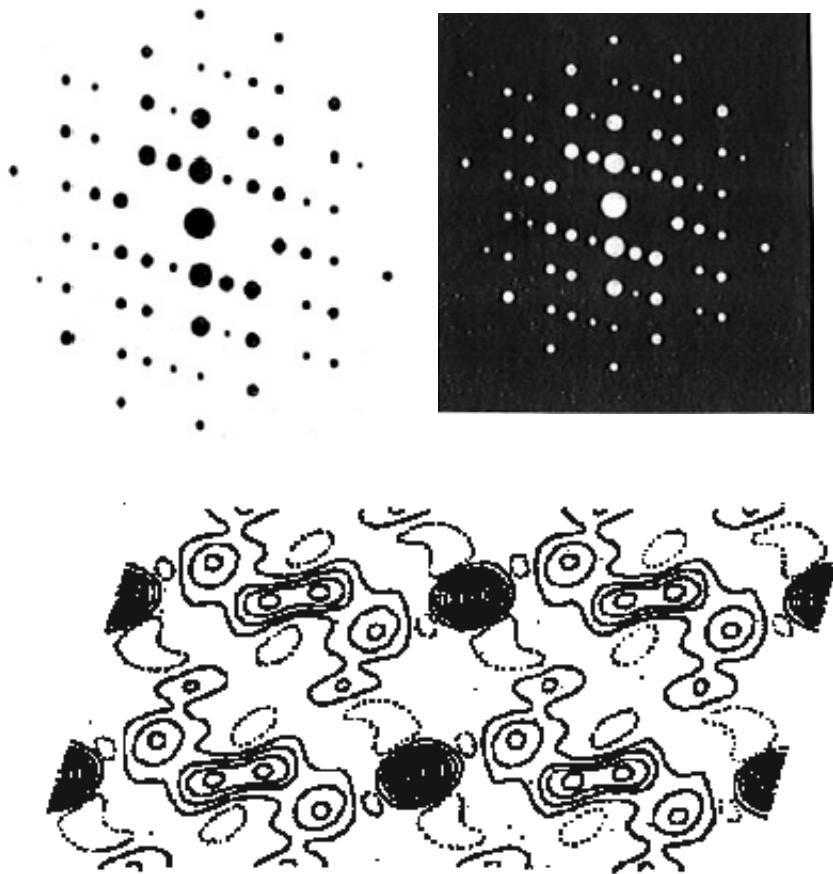


Rosalind Franklin's DNA "photo 51"



Bragg's "X-ray Microscope"

W.L.Bragg Nature, 143, 678 (1939): diopside, $\text{CaMg}(\text{SiO}_3)_2$



Arizona X-ray Pioneers



John Cowley
1923-2004



Steve Wilkins
1946-2013

Advanced Photon Source (ANL)

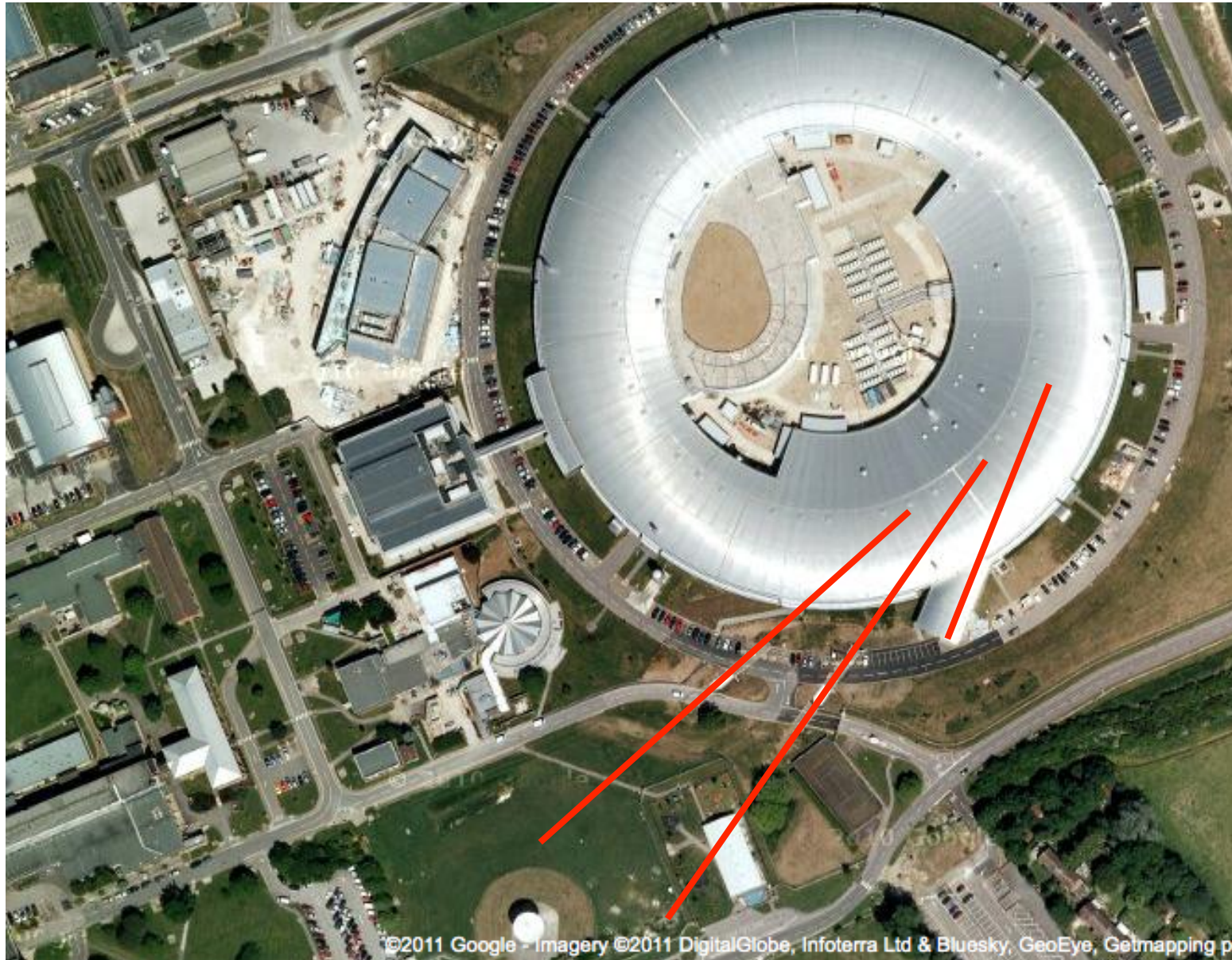
Urbana



34-ID-C

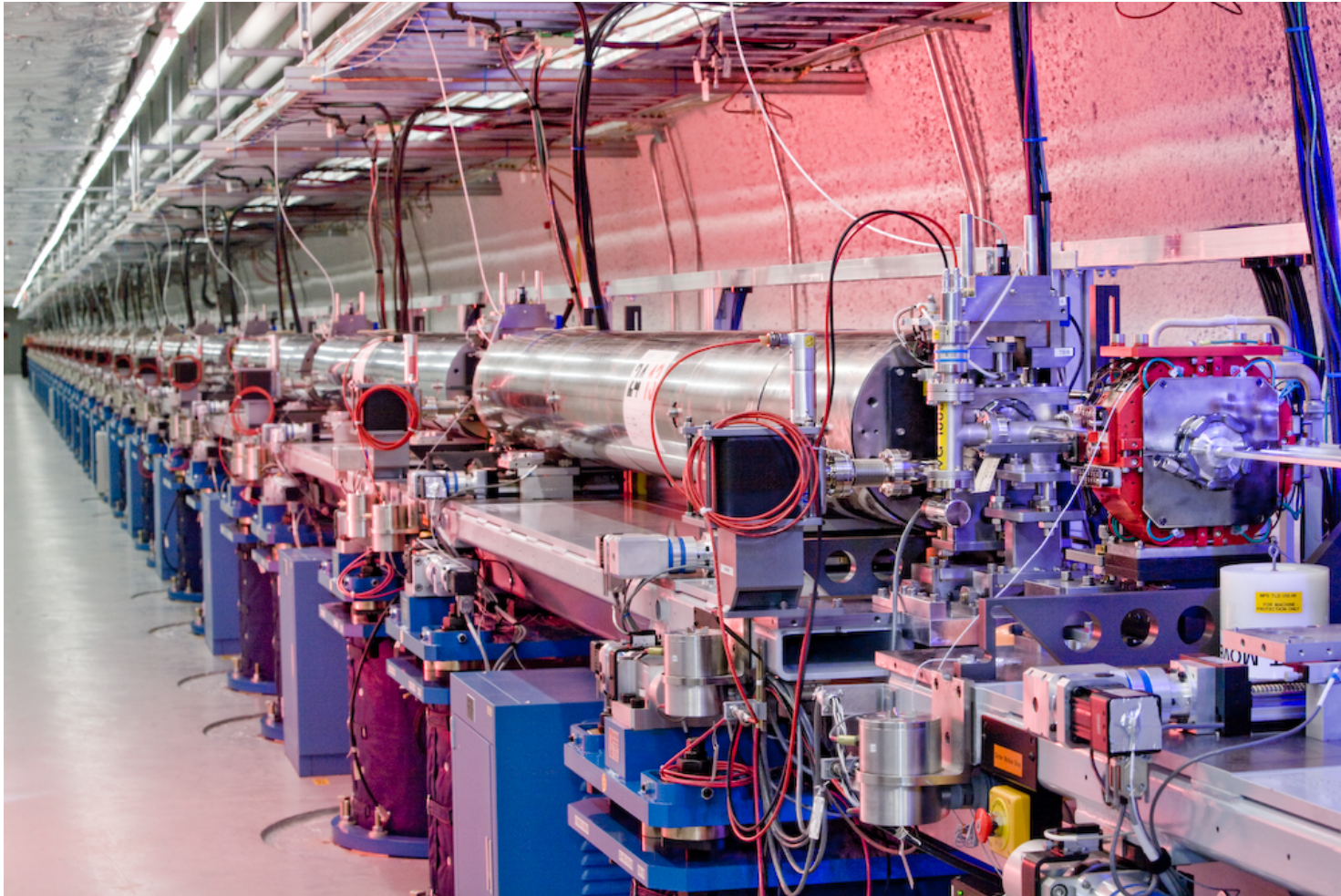


Diamond Light Source, 2009



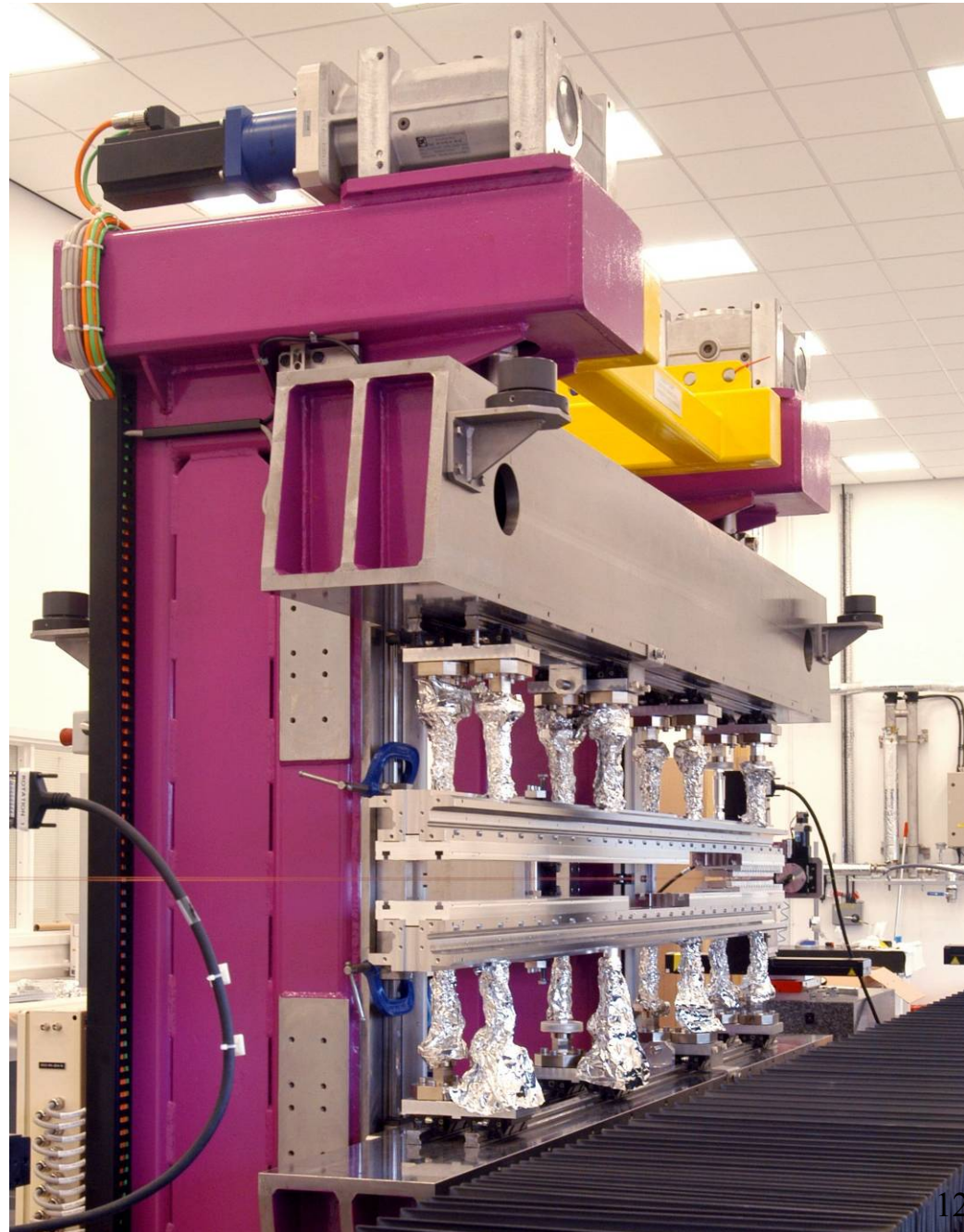
Linac Coherent Light Source

X-Ray Free-electron Laser, SLAC, Stanford, USA



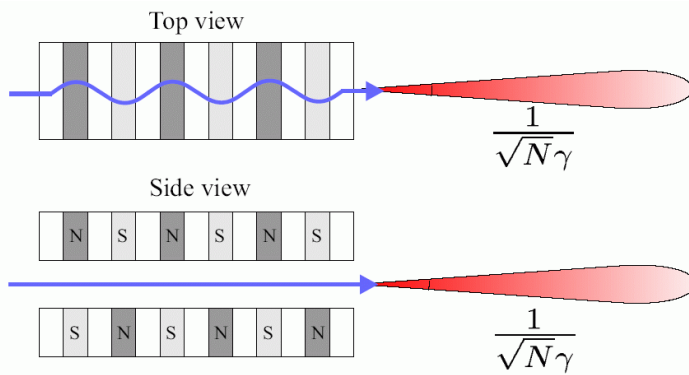
I. K. Robinson, ASU 2018

Diamond
in-vacuum
X-ray
Undulator



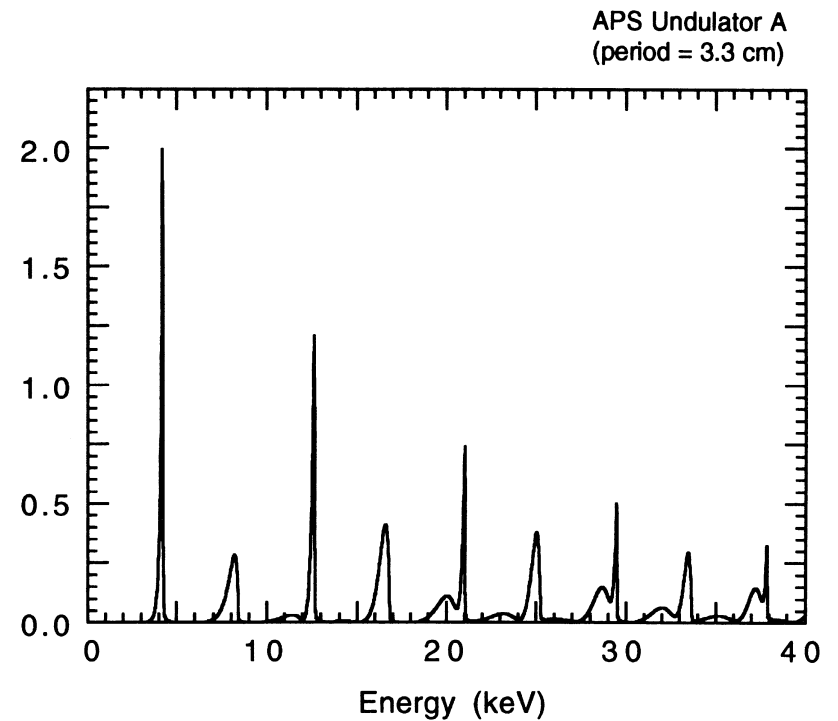
X-ray Undulator Principle

Vitalii Ginzburg, Novosibirsk (1947)

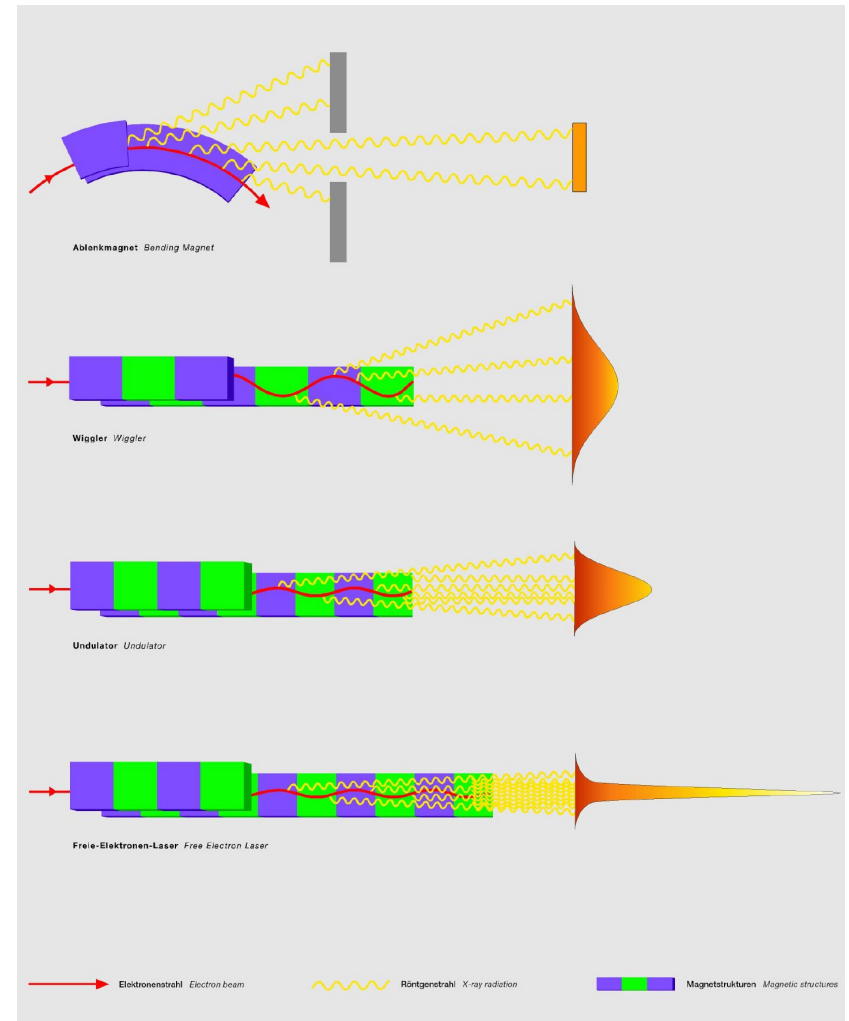
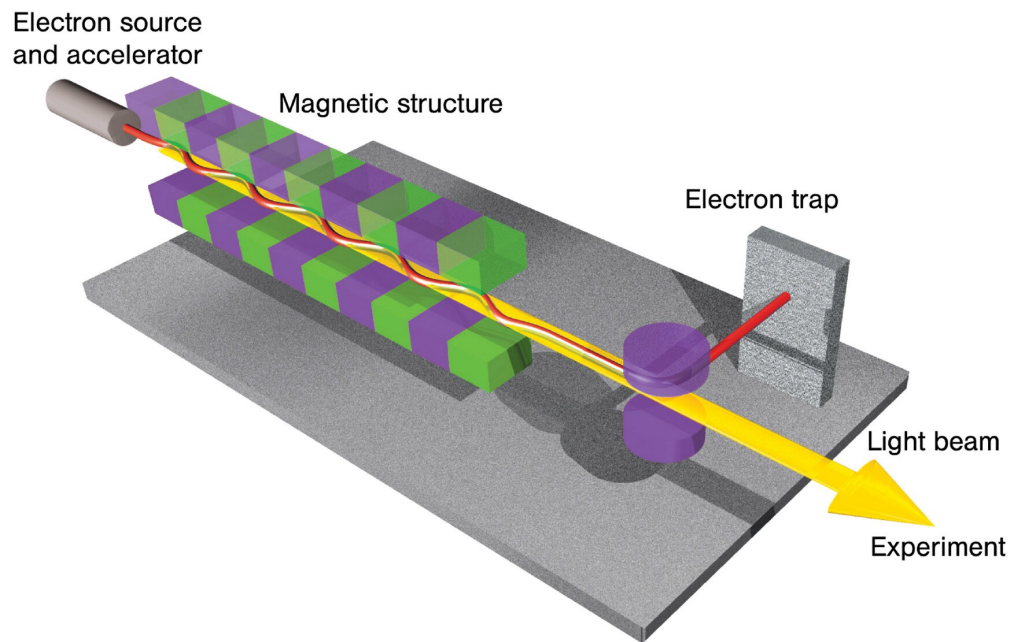


$$\lambda_X = \frac{\lambda_U}{2\gamma^2} \left\{ 1 + \frac{K^2}{2} + (\gamma\theta)^2 \right\}$$

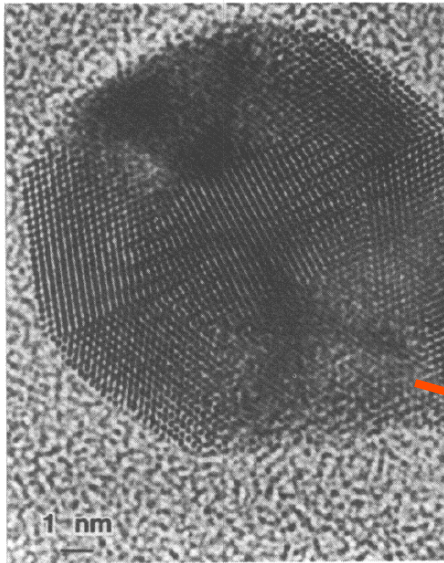
Brilliance ($\times 10^{18}$ ph/s/0.1%BW/mrad²/mm²)



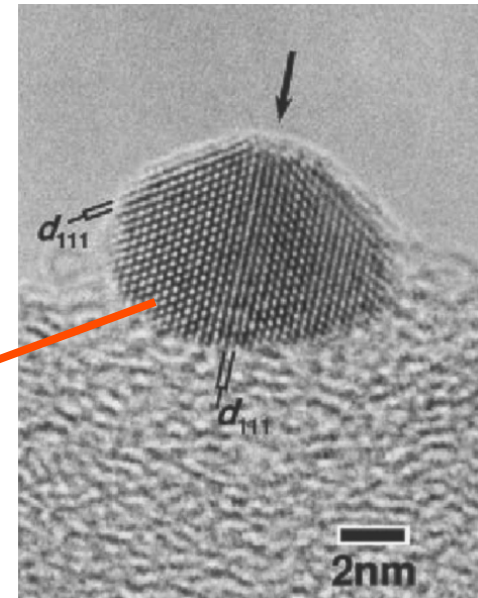
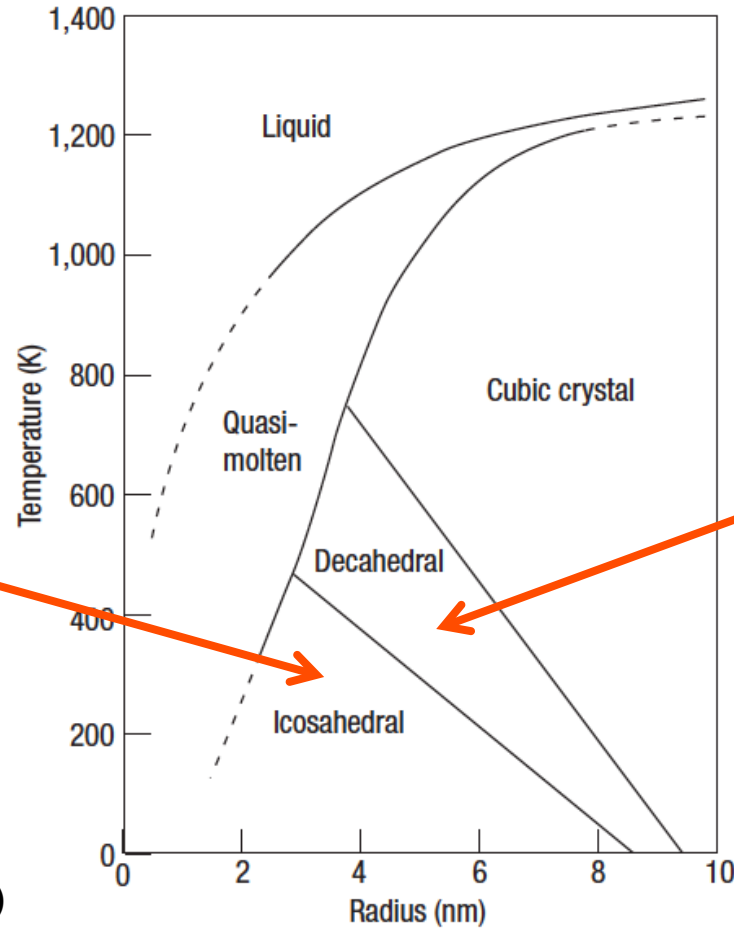
XFEL principle



Structure of Gold vs Size



L. D. Marks, RPP (1994)

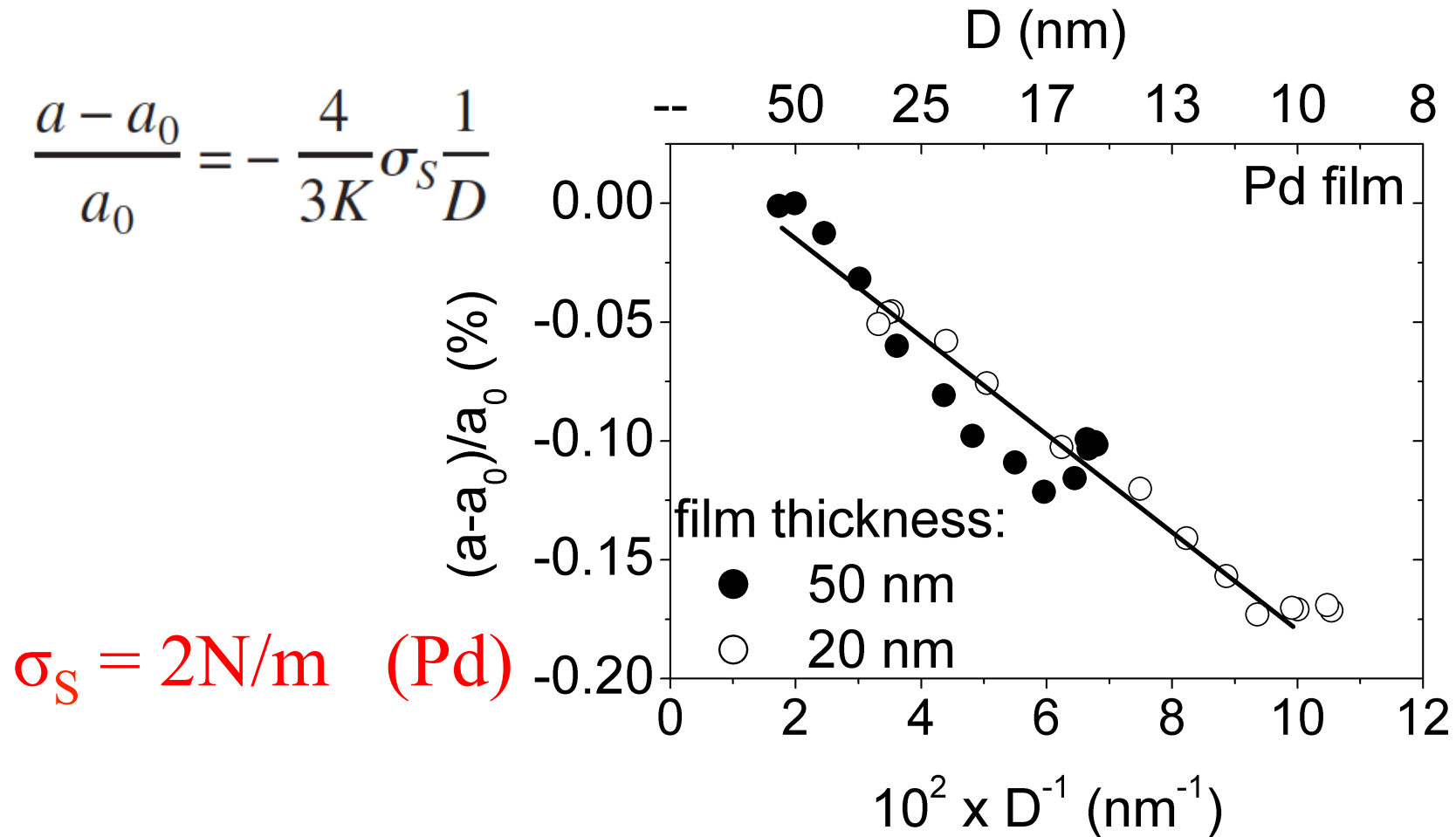


Koga and Sugawara (2003)

Contraction of Small Particles

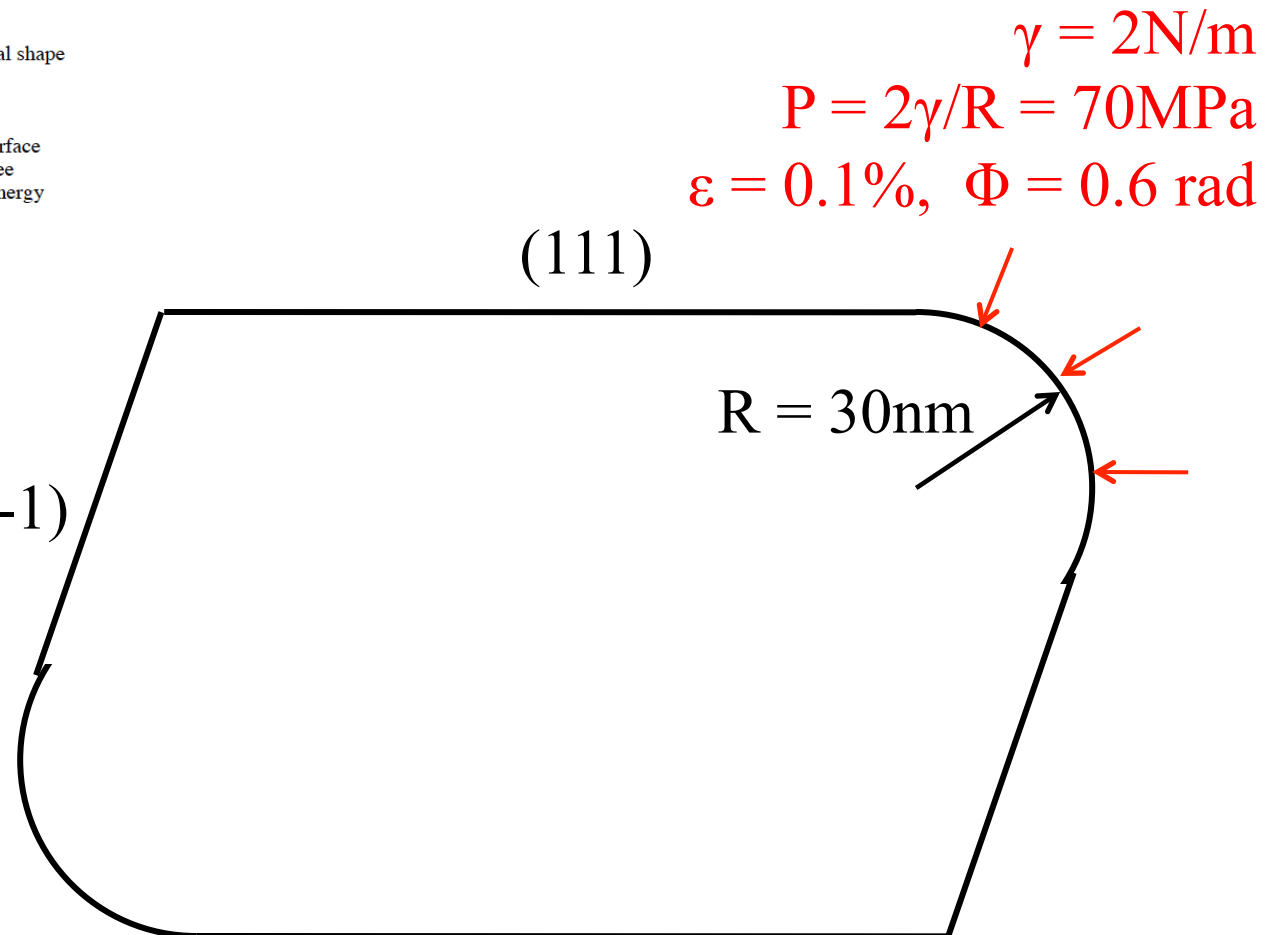
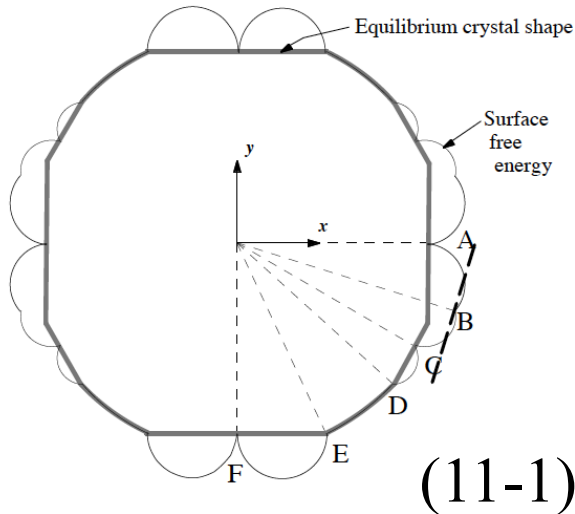
Gibbs Thomson pressure + Bulk modulus

Sheng, Welzel & Mittemeijer, APL 97 153109 (2010)

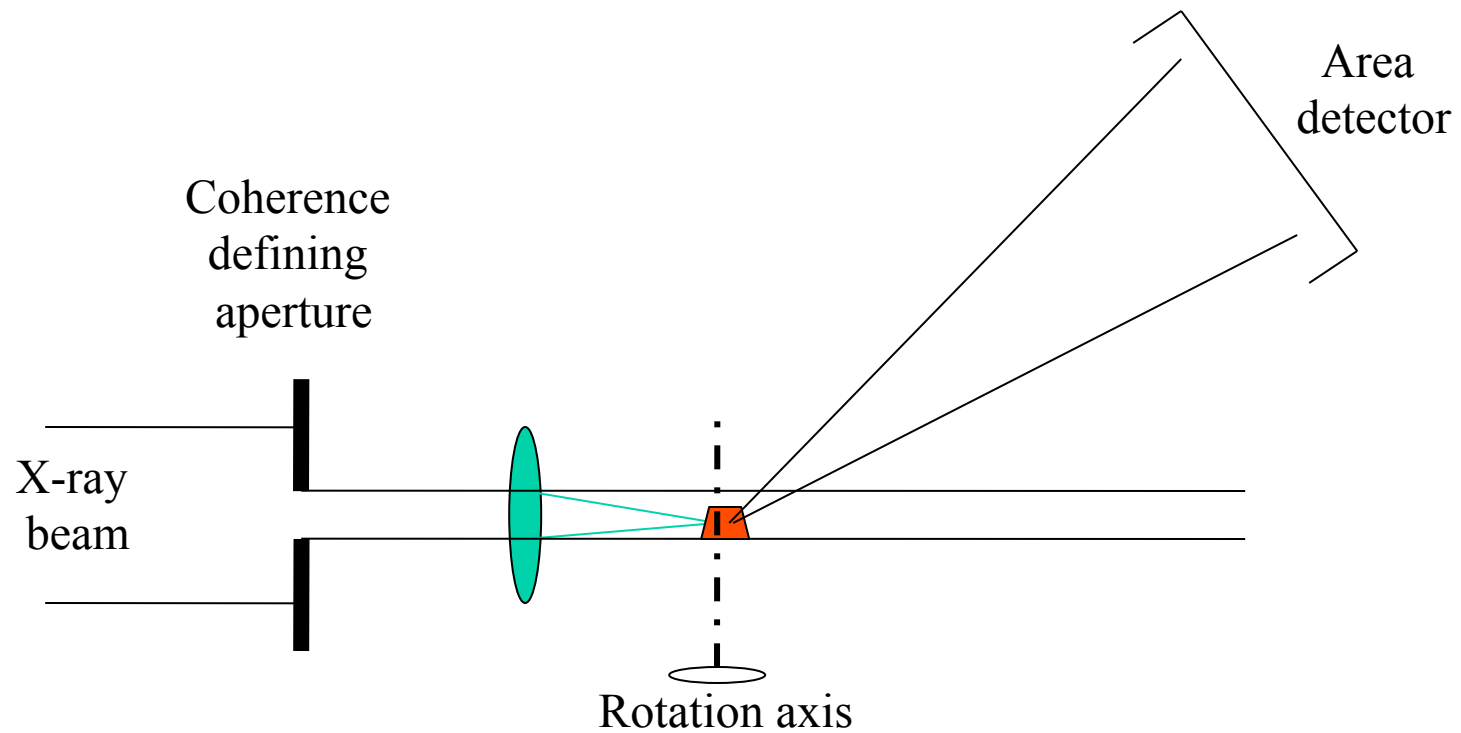


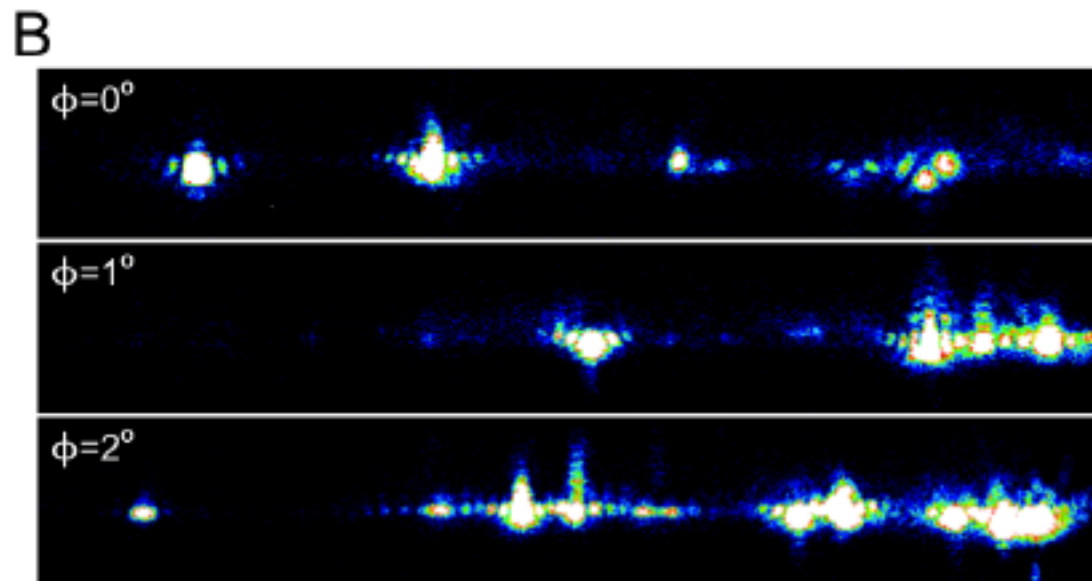
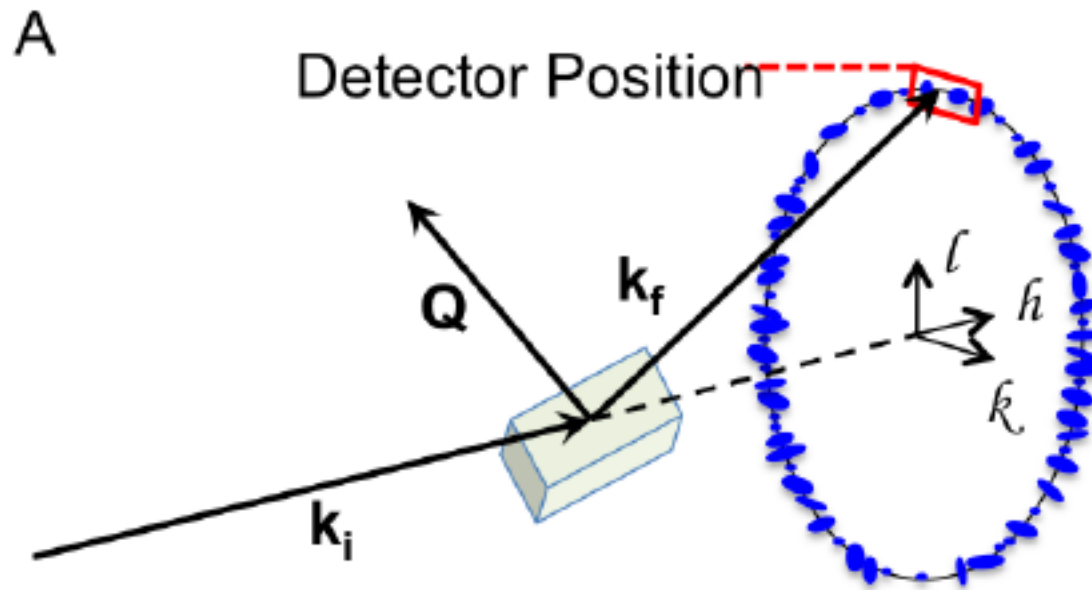
Equilibrium crystal shape

Wulff construction + Gibbs Thomson (Young-Laplace) pressure

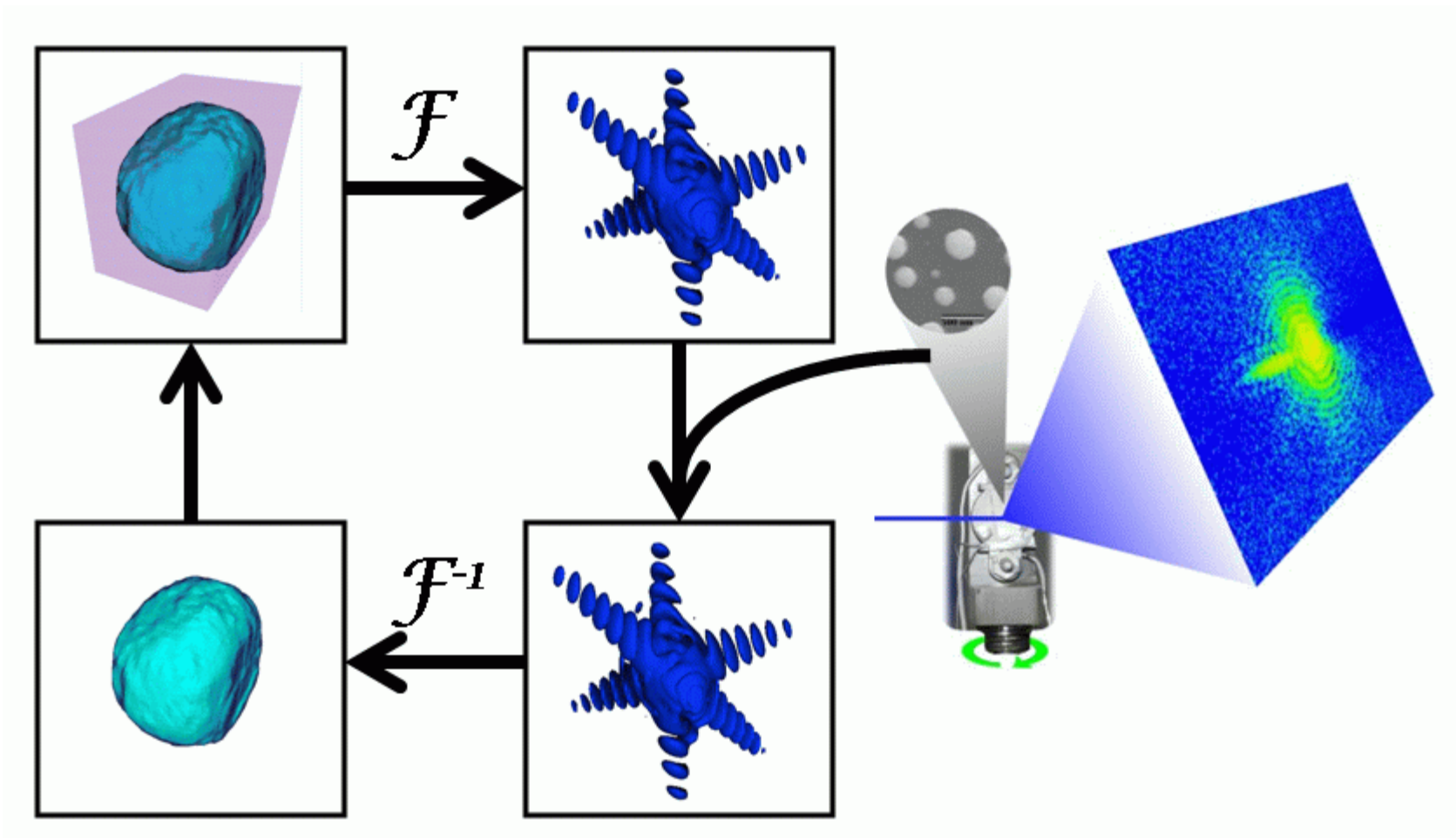


Lensless X-ray Microscope, 2003





Generic “Error Reduction” method



J. R. Fienup Appl. Opt. 21 2758 (1982)

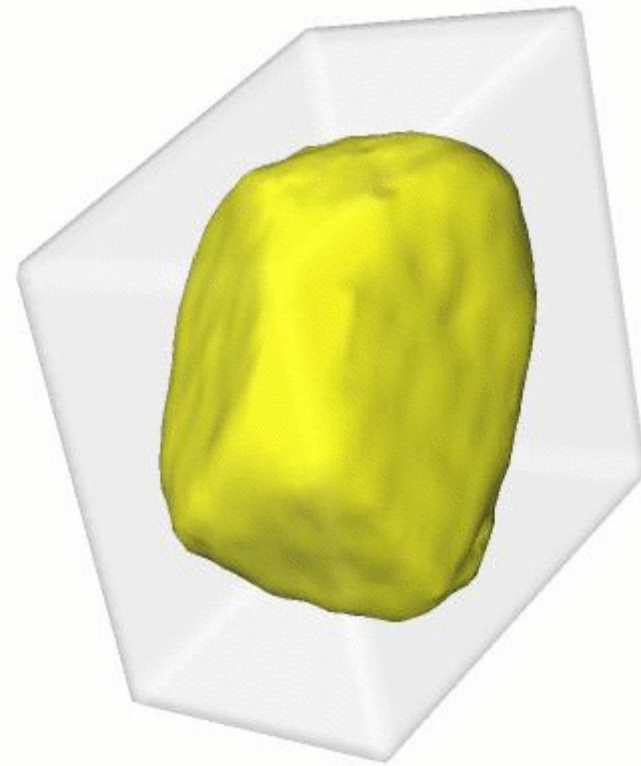
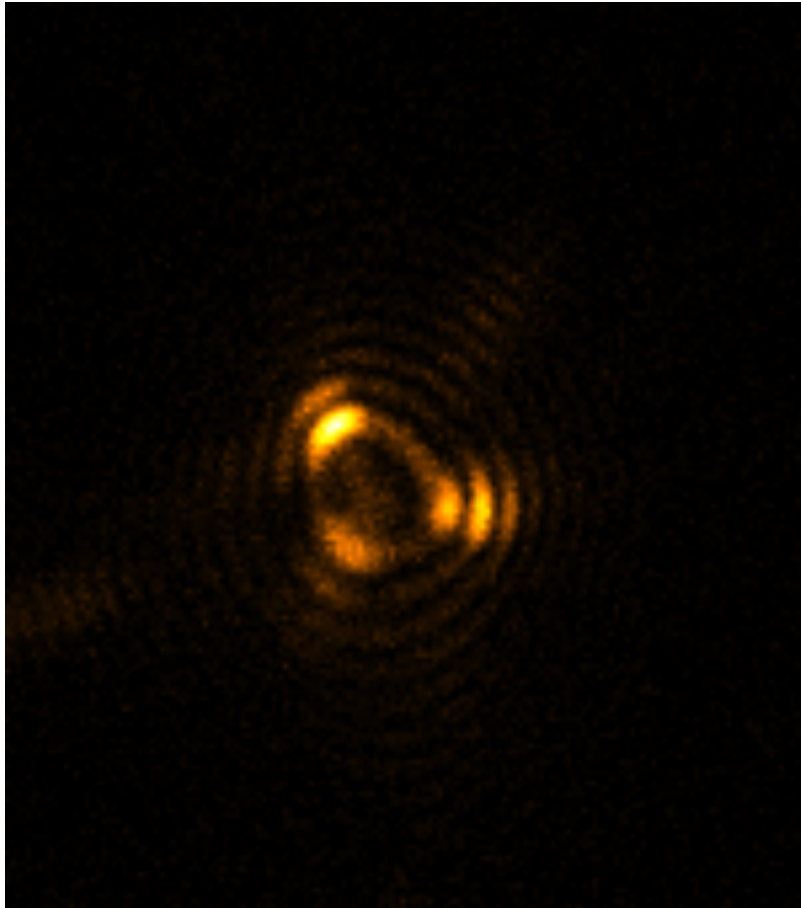
R. W. Gerchberg and W. O. Saxton Optik 35 237 (1972)

I. K. Robinson, ASU 2018

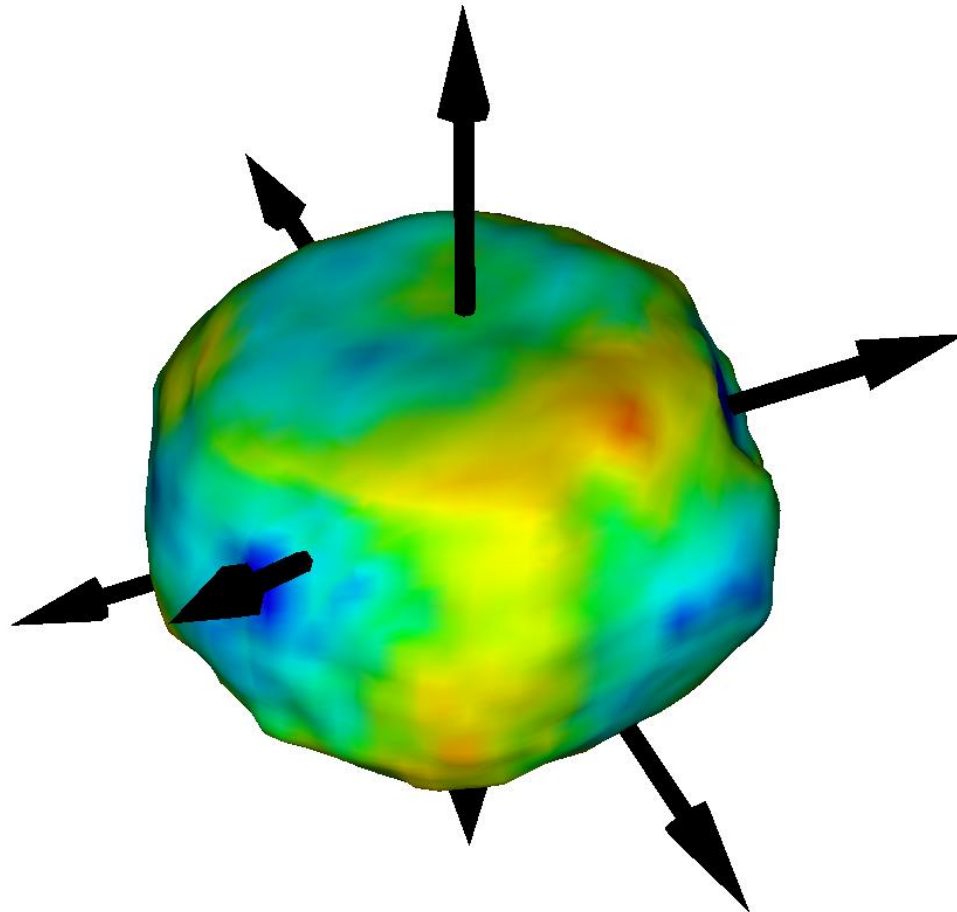
20

Gold nanocrystal reconstruction

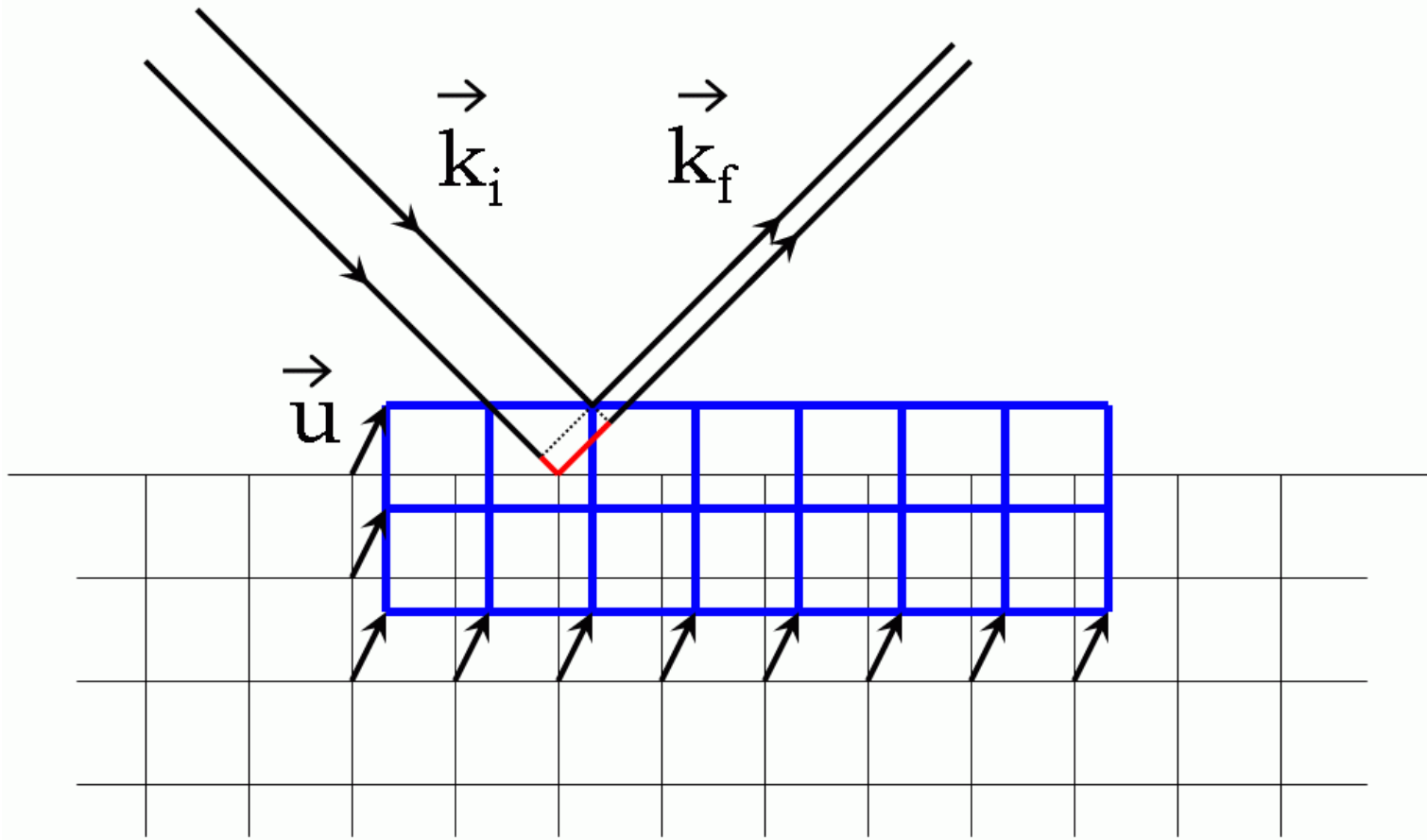
showing support used for 20 HIO followed by 10 ER



Phase isosurface of residual strain

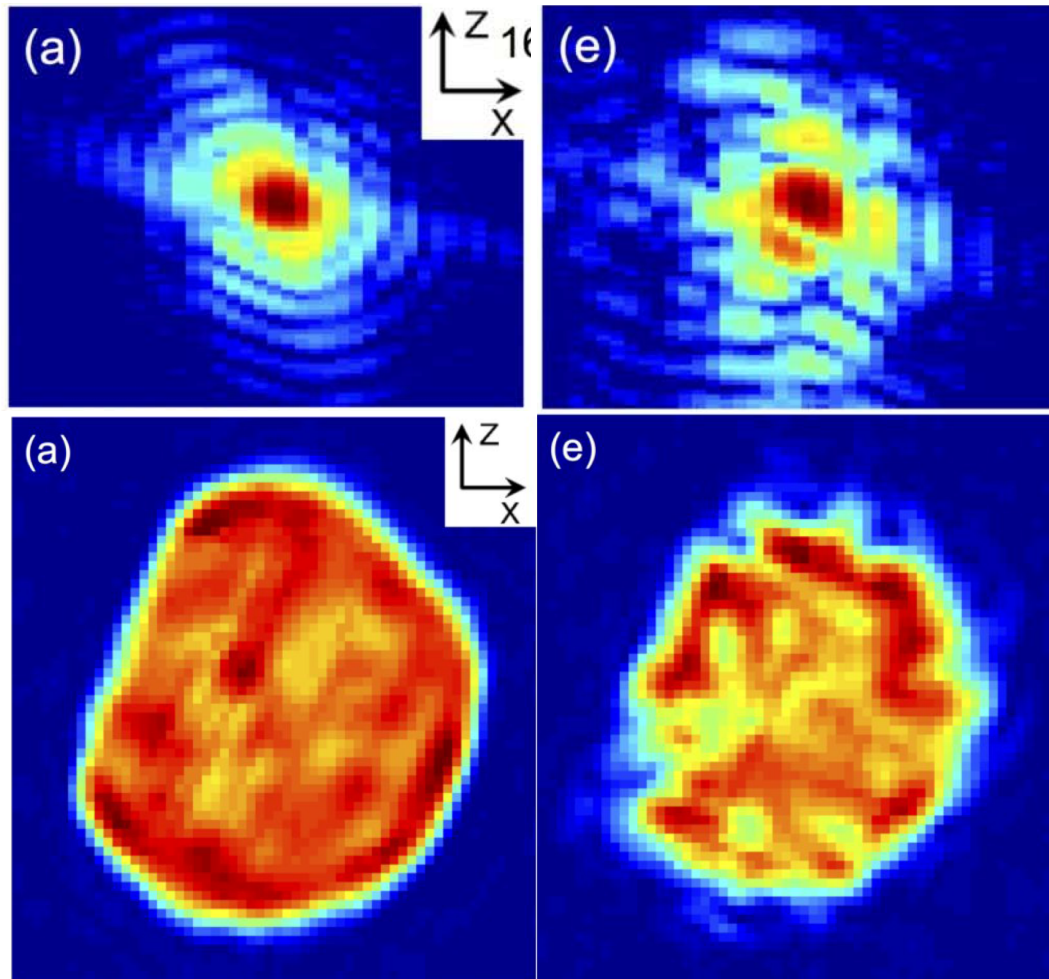


Sensitivity to strain

$$\Delta\varphi = \mathbf{k}_f \cdot \mathbf{u} - \mathbf{k}_i \cdot \mathbf{u} = \mathbf{Q} \cdot \mathbf{u}$$


Copper Diffusion into Gold Nanocrystal

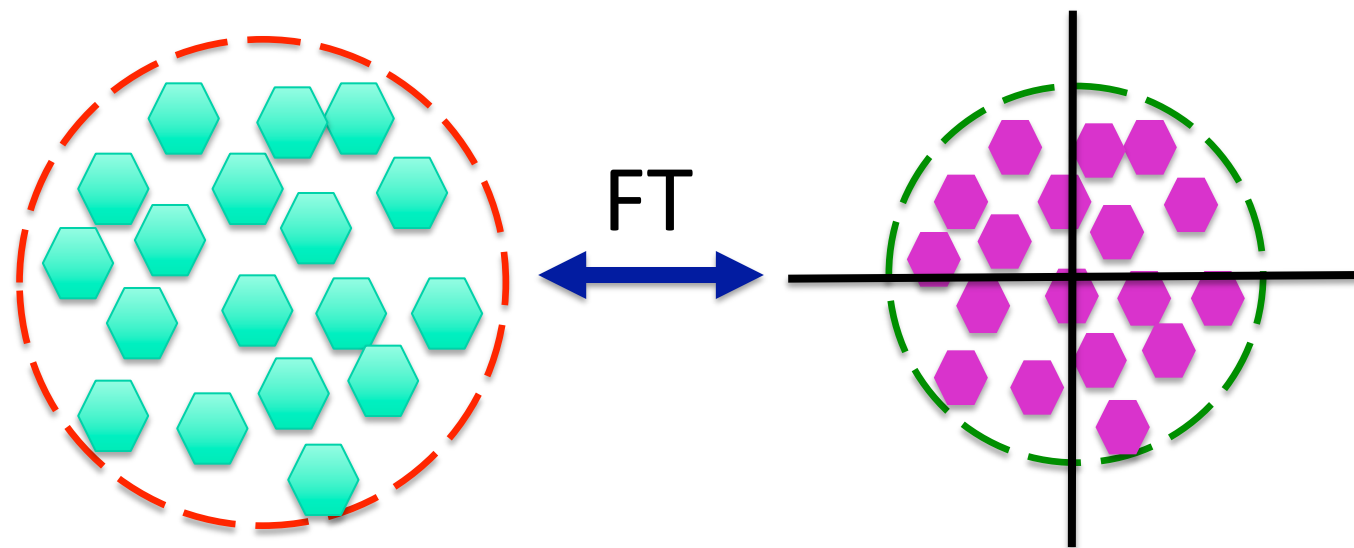
Gang Xiong, et al, Sci Rep 4 6765 (2013)

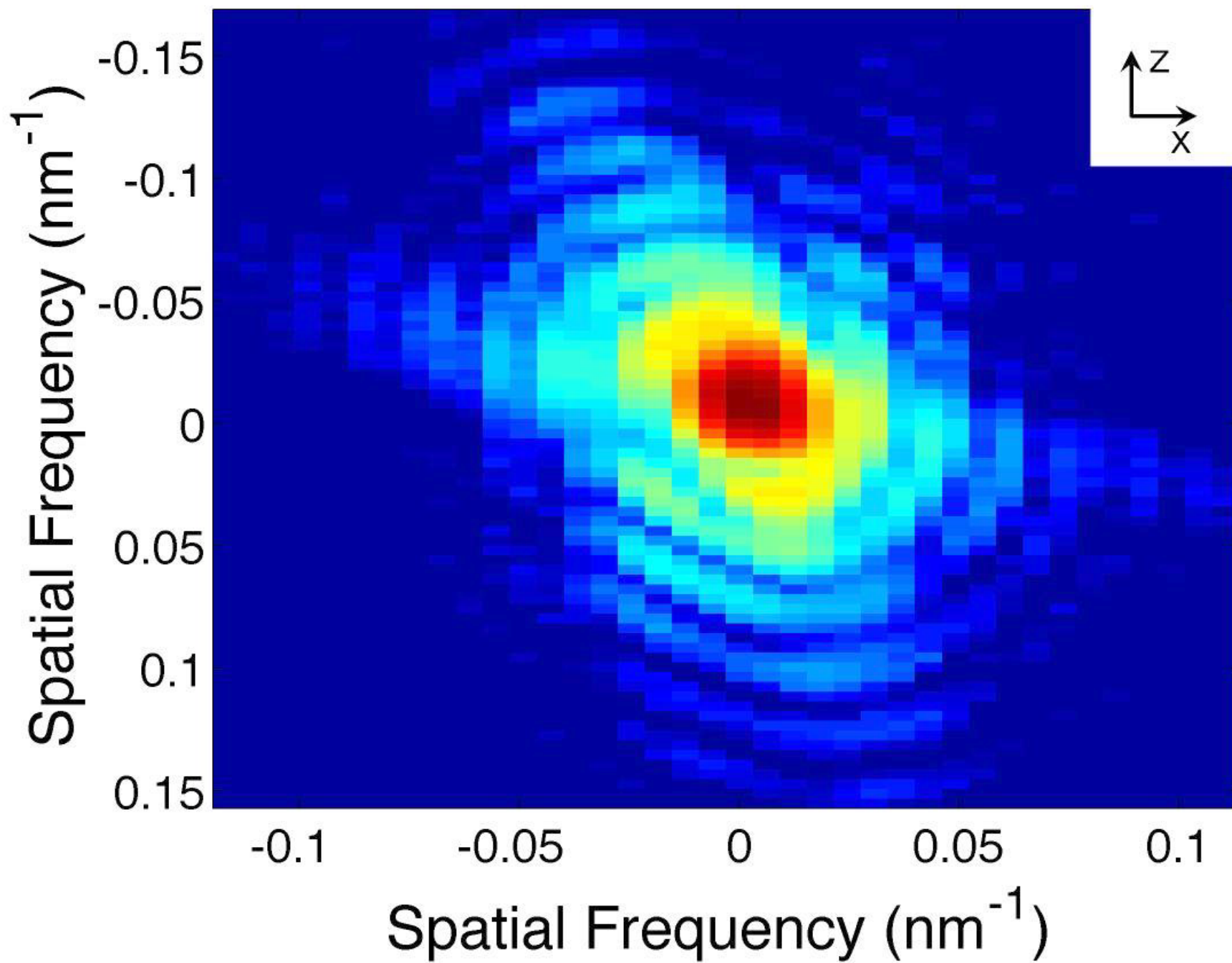


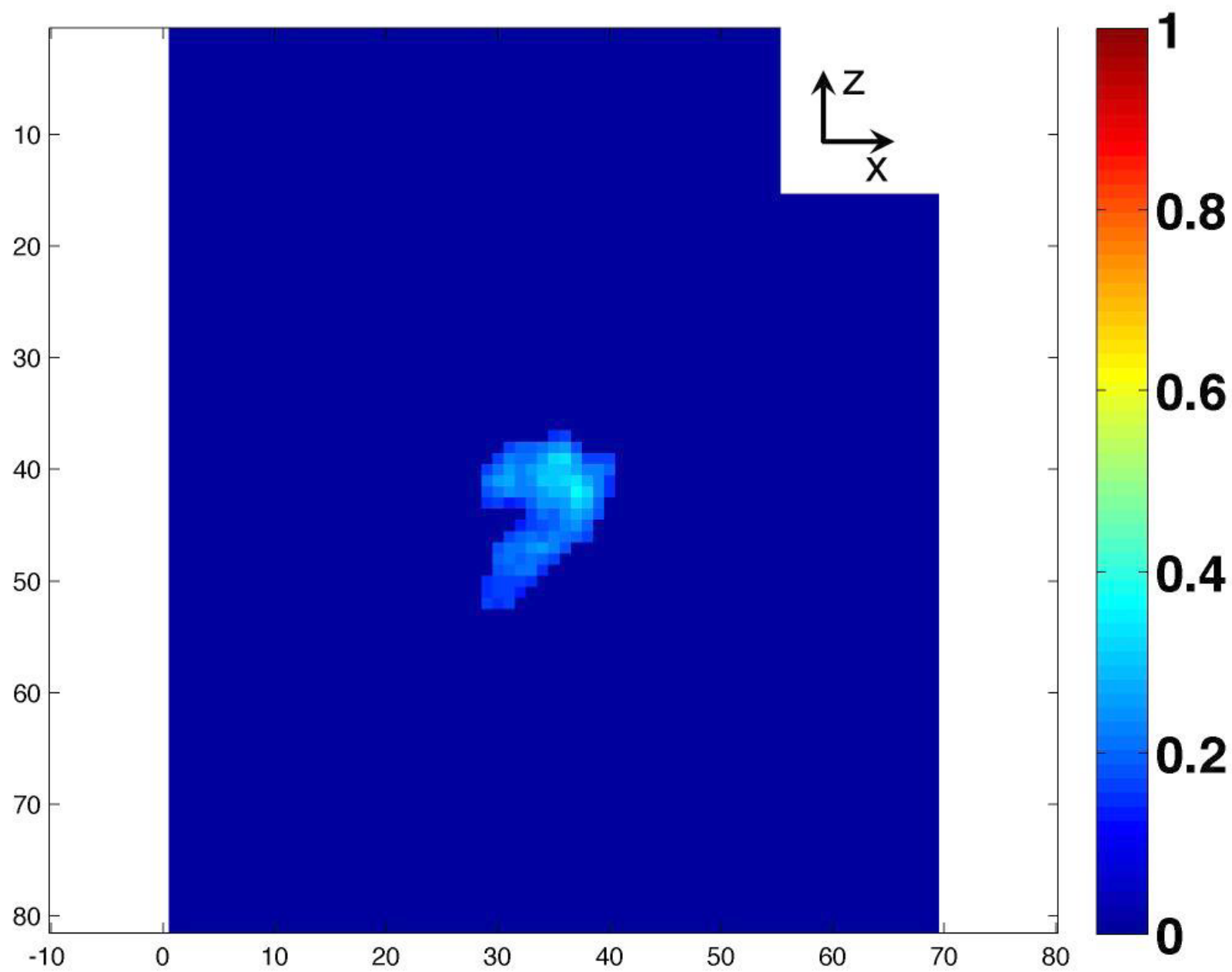
Domain structures give speckled diffraction

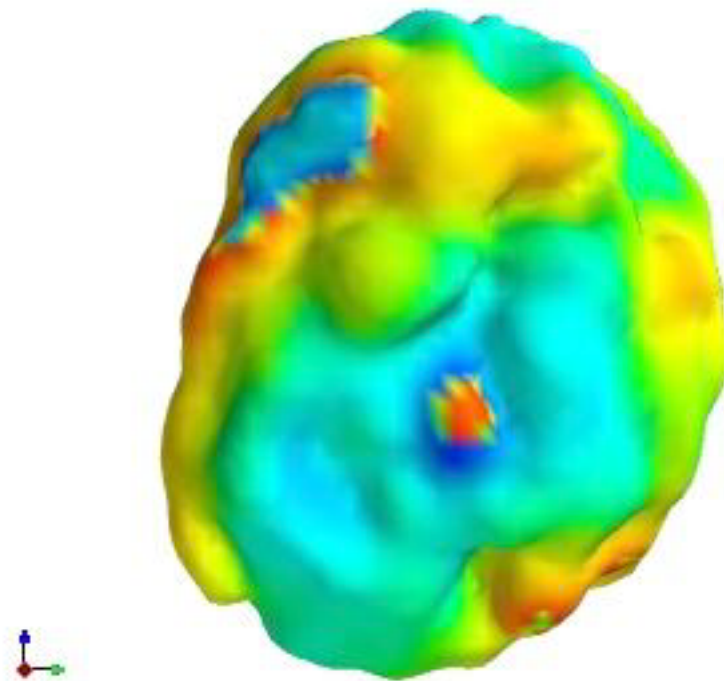
Real Space

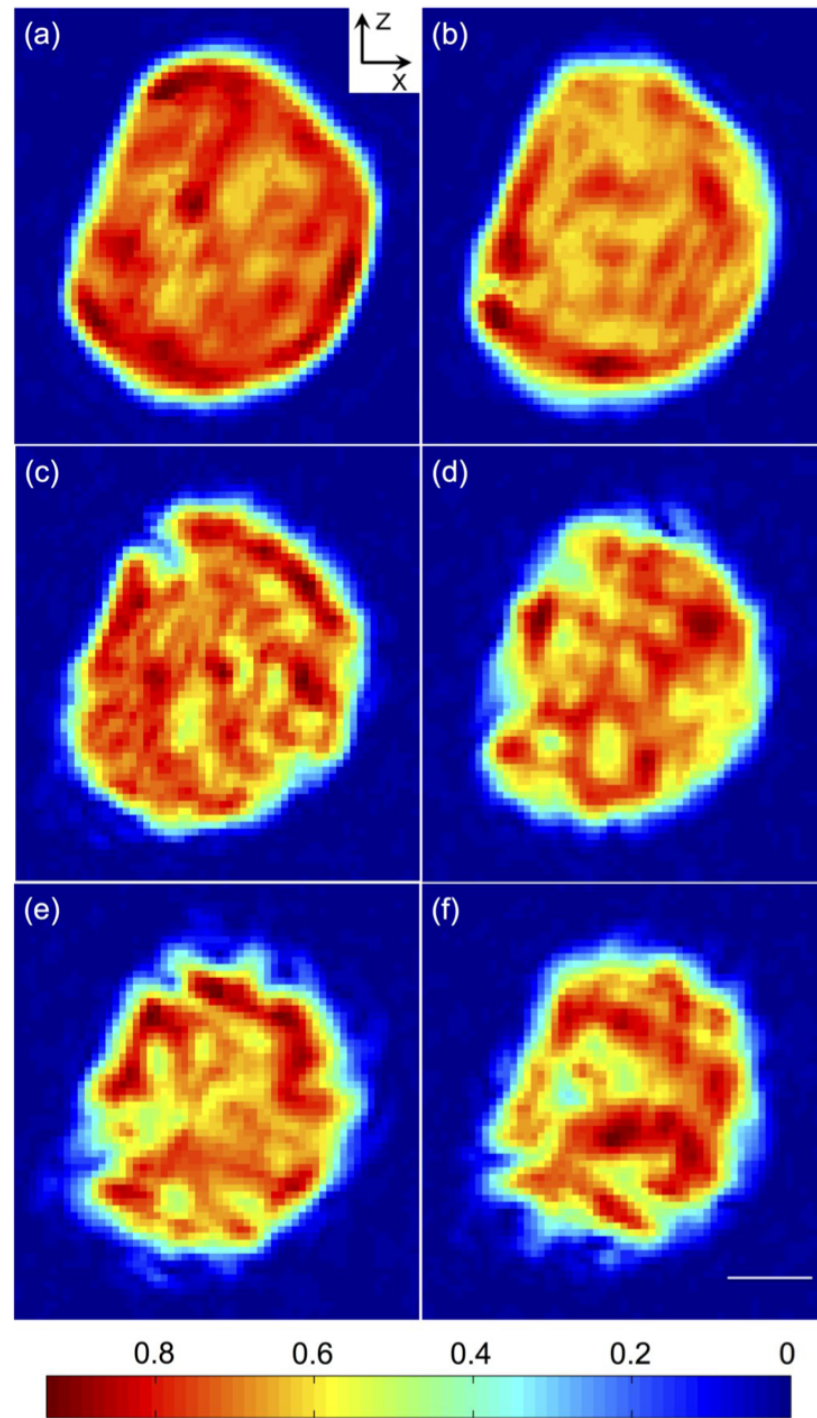
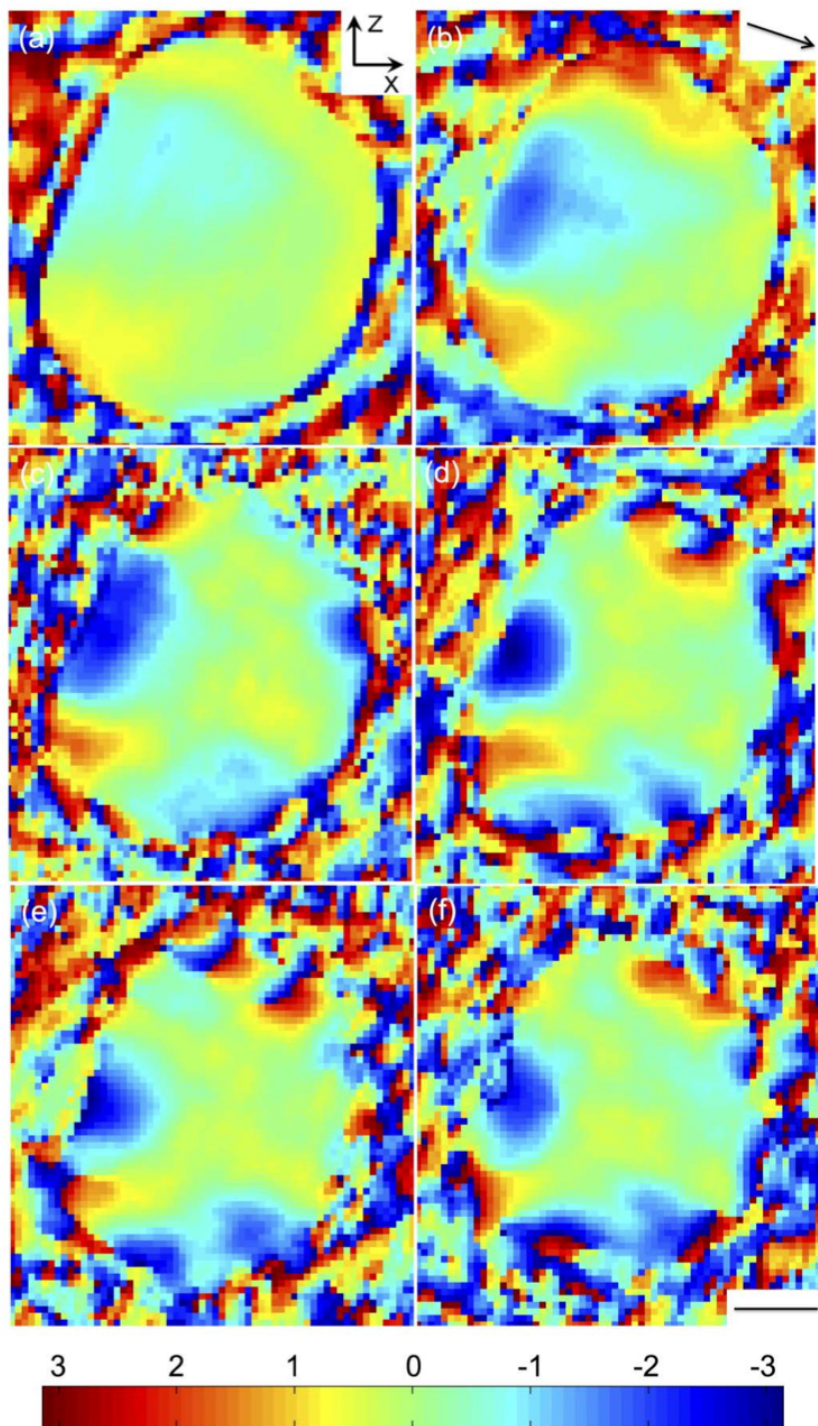
Reciprocal Space





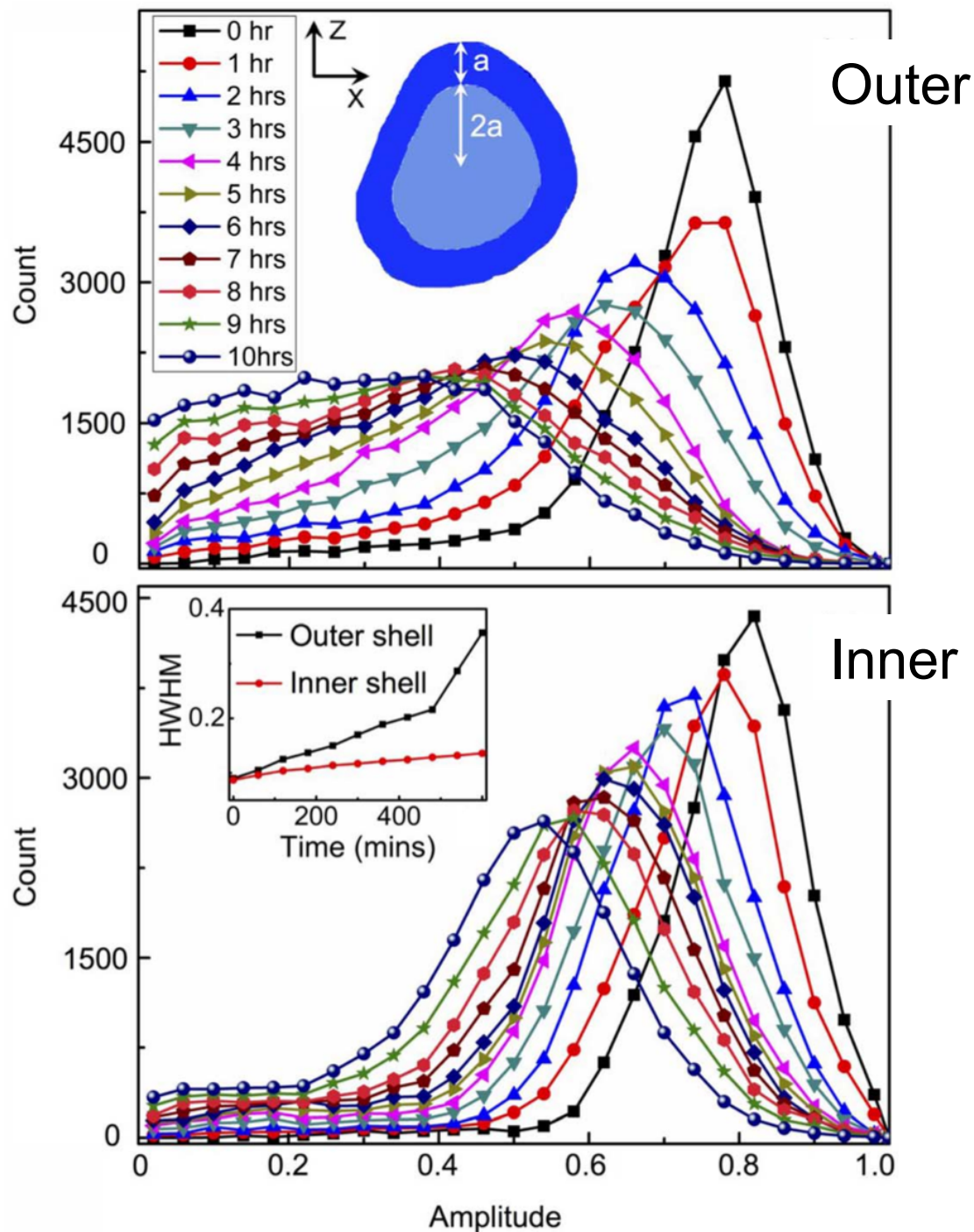






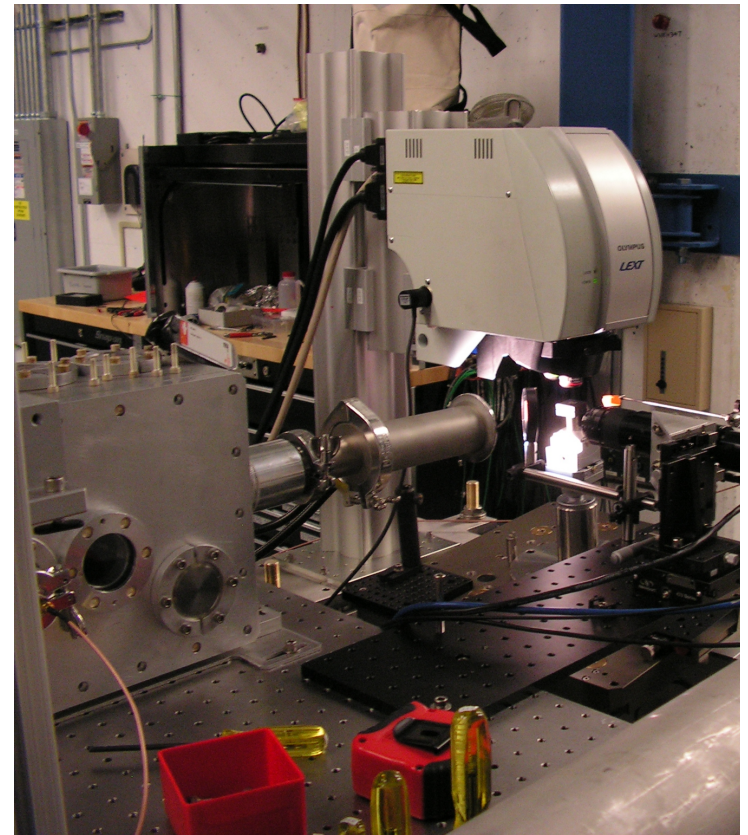
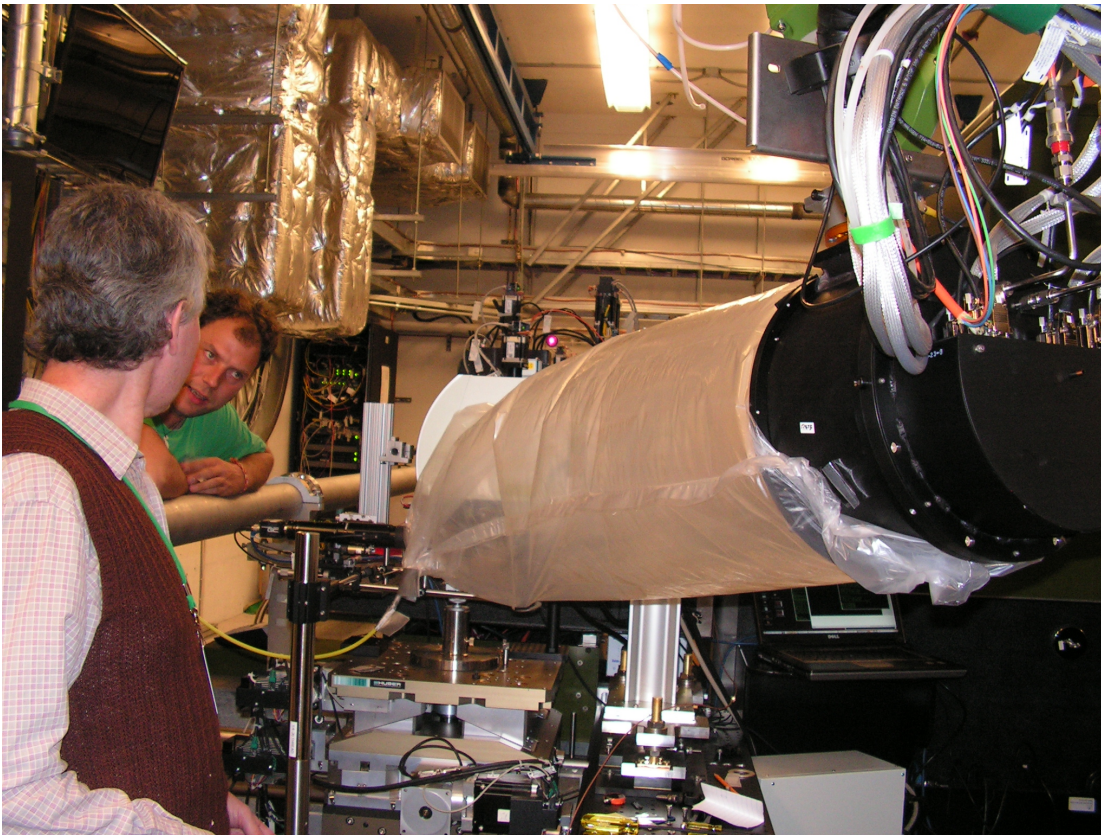
Atomic Diffusion within Individual Gold Nanocrystal

Gang Xiong,
J. N. Clark,
C. Nicklin,
J. Rawle &
I. K. Robinson
Sci Rep 4 6765
(2013)

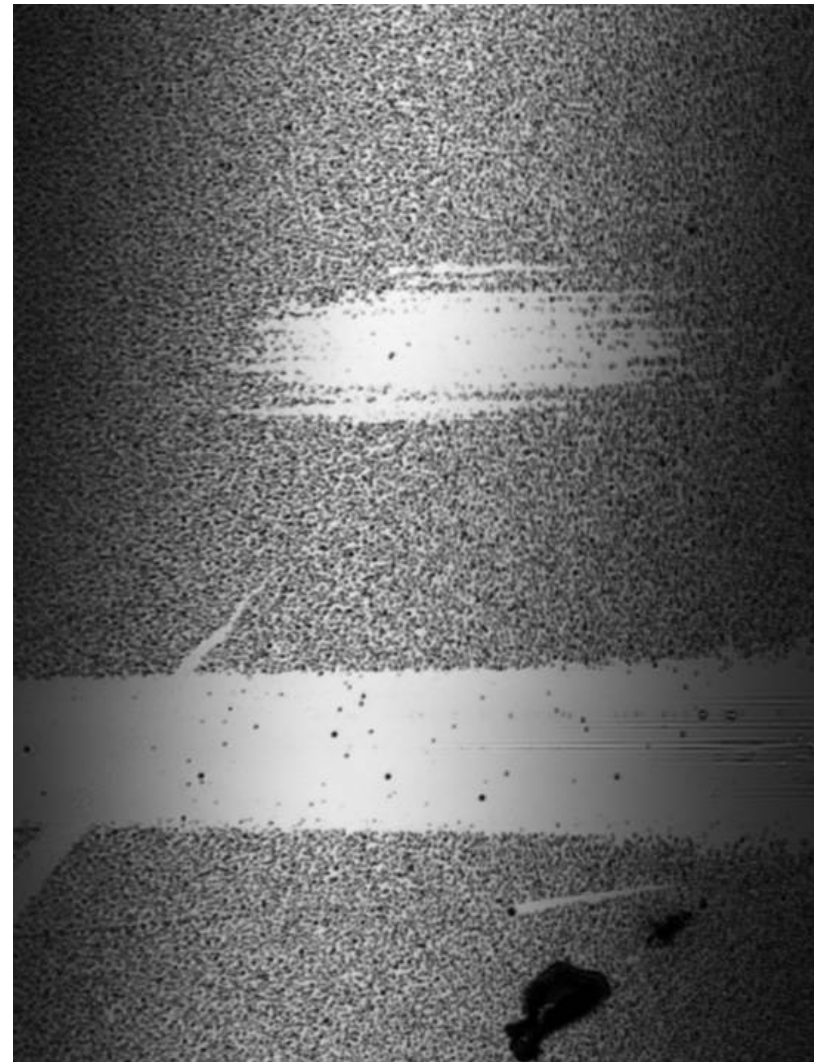
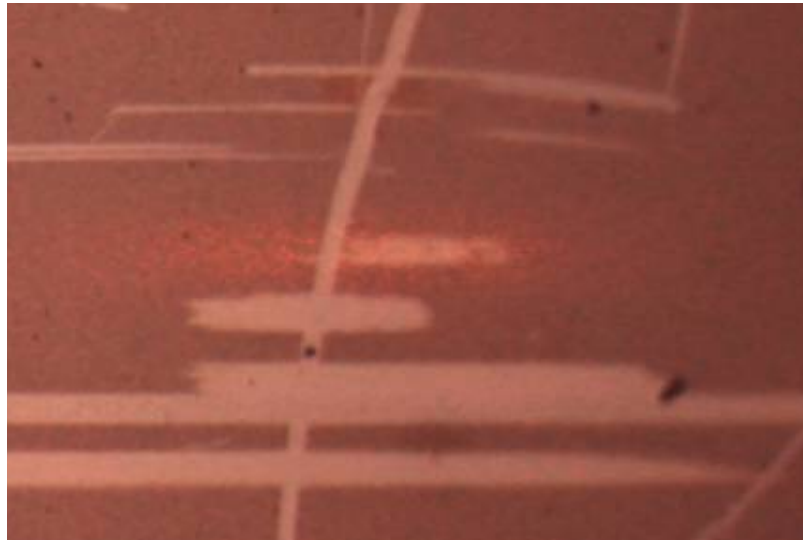


Pump-probe at LCLS (XPP)

Justin Wark, Loren Beitra, Alexander Korsunsky, Ross Harder, David Fritz ,
Sebastien Boutet, Jesse Clark, Garth Williams, Brian Abbey, Andy Higginbotham,
Diling Zhu, Henrick Lemke, Mattieu Chollet, Marc Messerschmidt

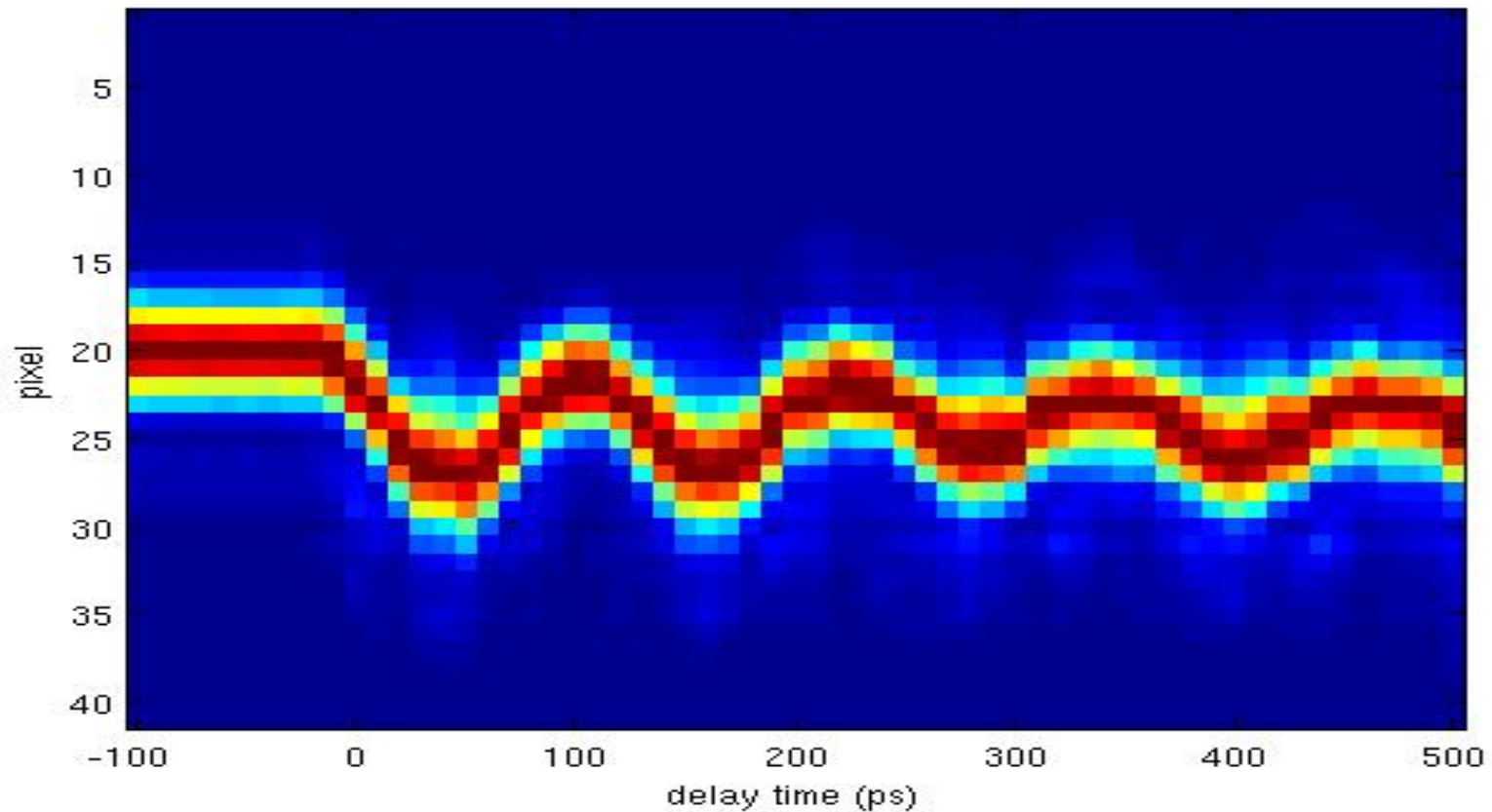


Visible and Confocal microscopy



Pump-probe at LCLS (XPP)

Justin Wark, Loren Beitra, Alexander Korsunsky, Ross Harder, David Fritz ,
Sebastien Boutet, **Jesse Clark**, Garth Williams, Brian Abbey, Andy Higginbotham,
Diling Zhu, Henrick Lemke, Mattieu Chollet, Marc Messerschmidt



“Two-temperature” model

Y. Ishida et al, Nature Scientific Reports 1 64 (2011)

J.K. Chen et al, Int J. Heat Transfer 49 307 (2006)

(a) Two-temperature model

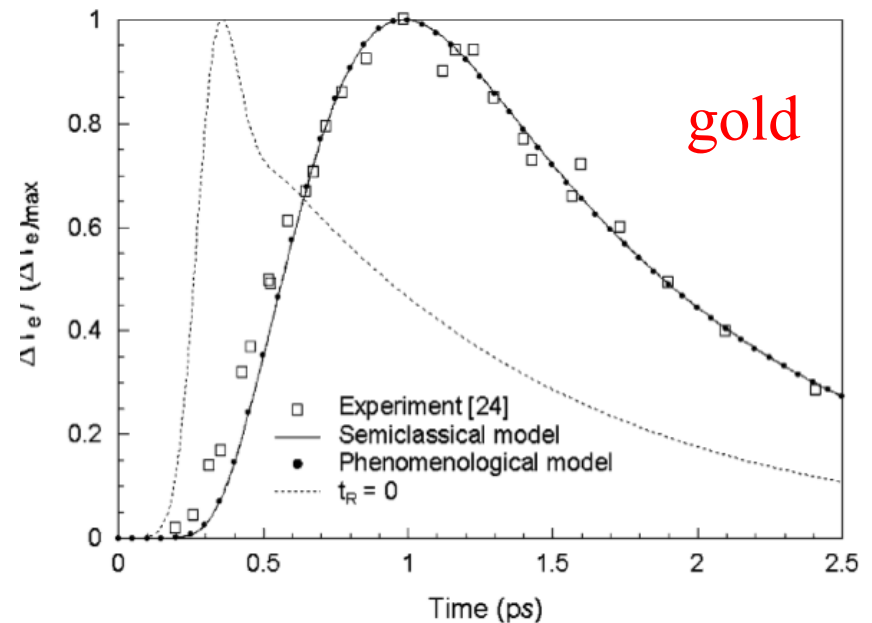
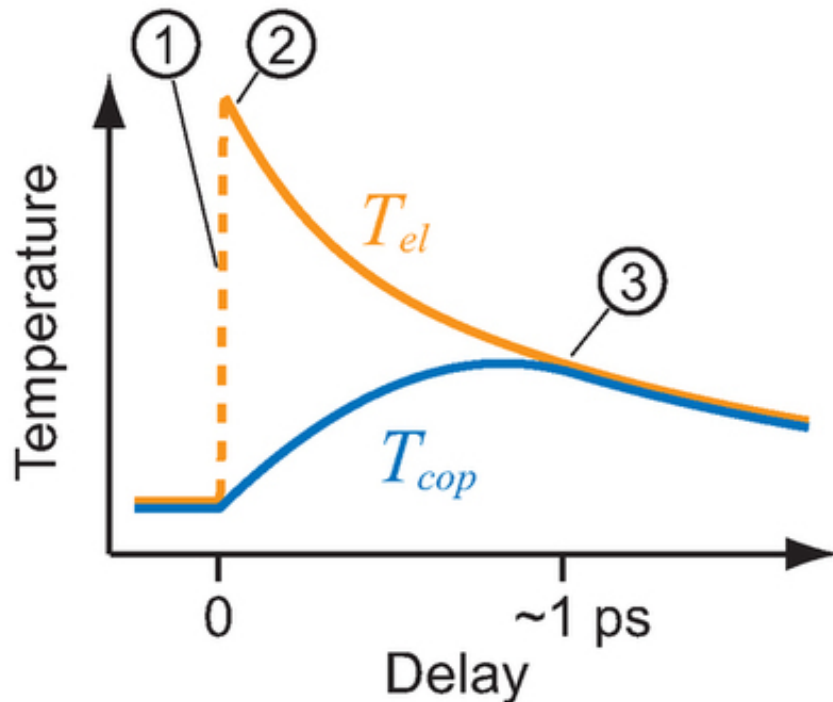
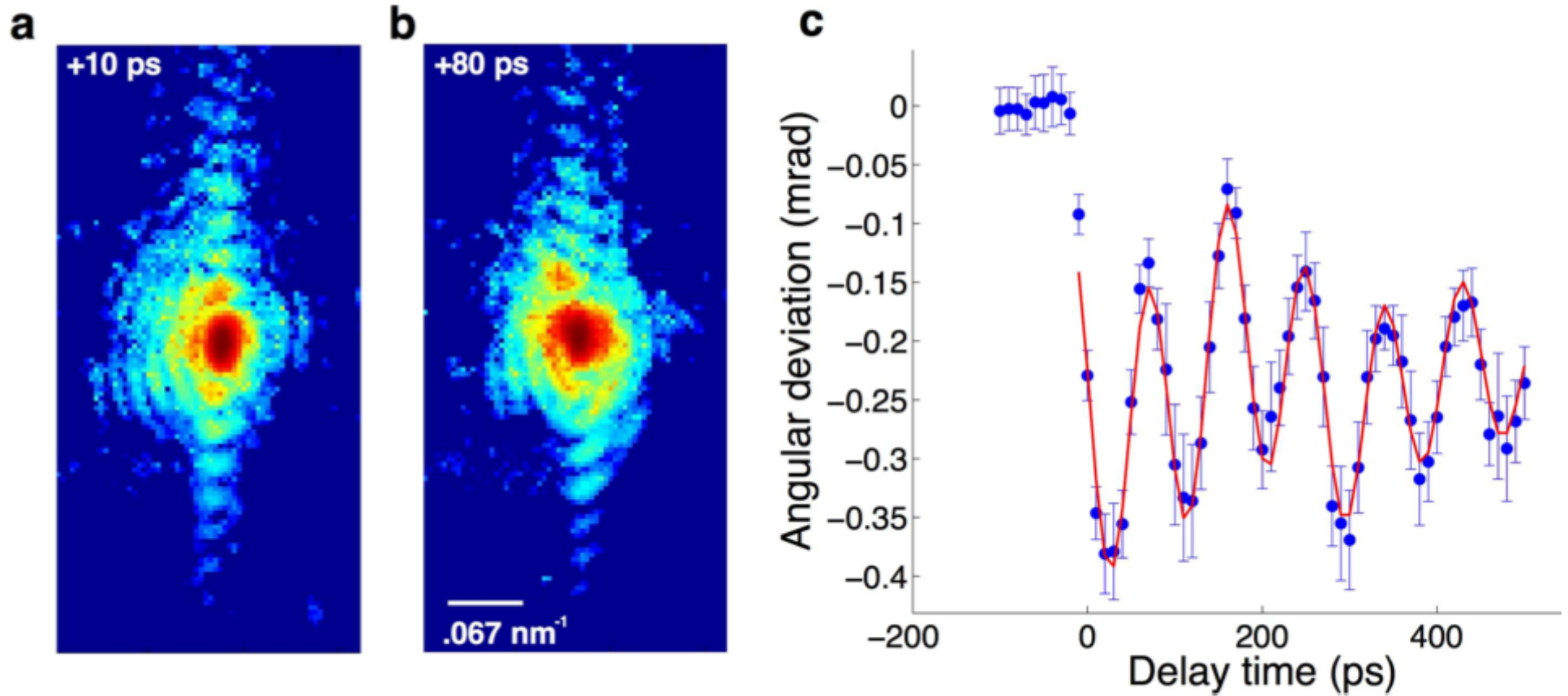


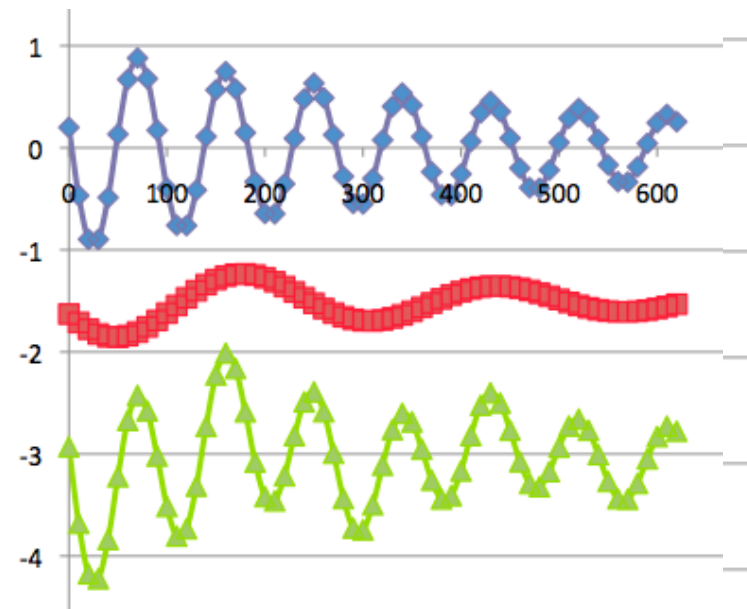
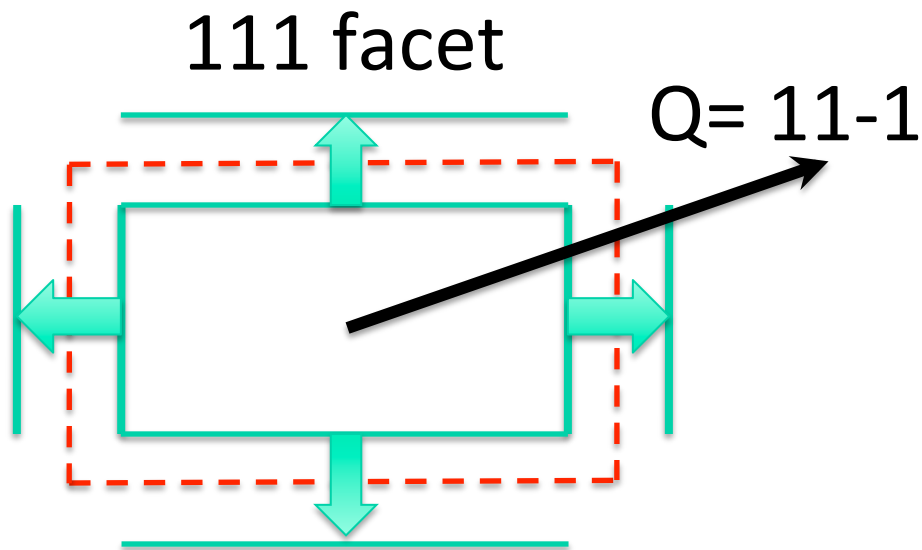
fig. 2. Comparison of the change in electron temperature at the front surface of an 80-nm gold film irradiated by a 2.8 mJ/n², 800 nm, 150-fs laser pulse.

Time resolved Bragg peak position



Two Normal Modes of Vibration

$$S(\tau) = \sum_{n=1}^N A_n \exp[-(\tau/\tau_{d,n})^2] \cos(\omega_n \tau + \varphi_{0,n})$$



$$T_1 = 90\text{ps} \quad h_1 = 145\text{nm} \quad c_S = 3240\text{ m/s}$$

$$T_2 = 259\text{ps} \quad h_2 = 420\text{nm}$$

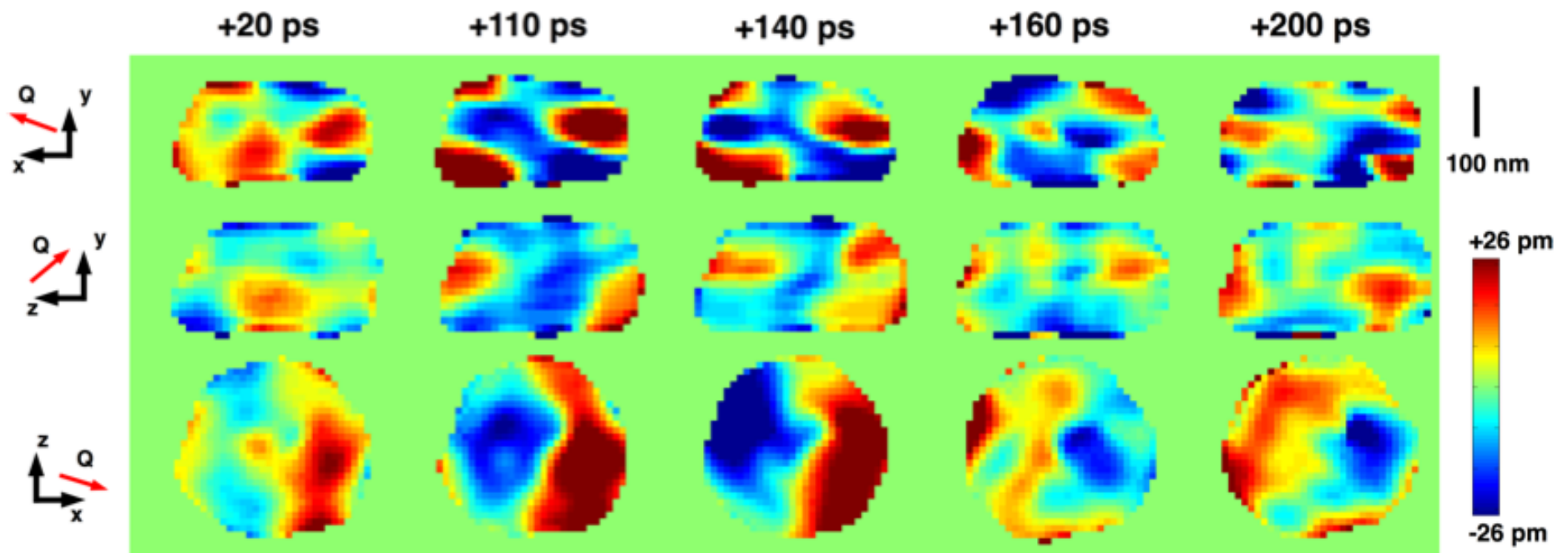
J. K. Robinson, ASU 2018

Dynamic imaging of displacements

CDI inversion of 3D diffraction patterns

1000 frames averaged at each point of rocking curve

Jesse Clark et al, Science 341 56 (2013)

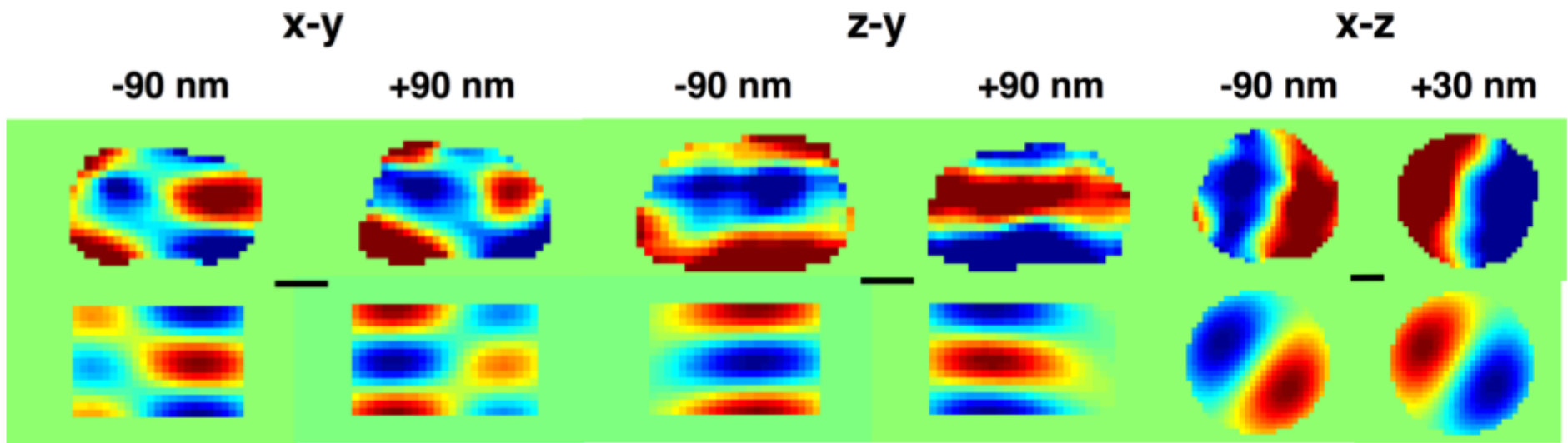


Dynamic imaging of displacements

CDI inversion of 3D diffraction patterns

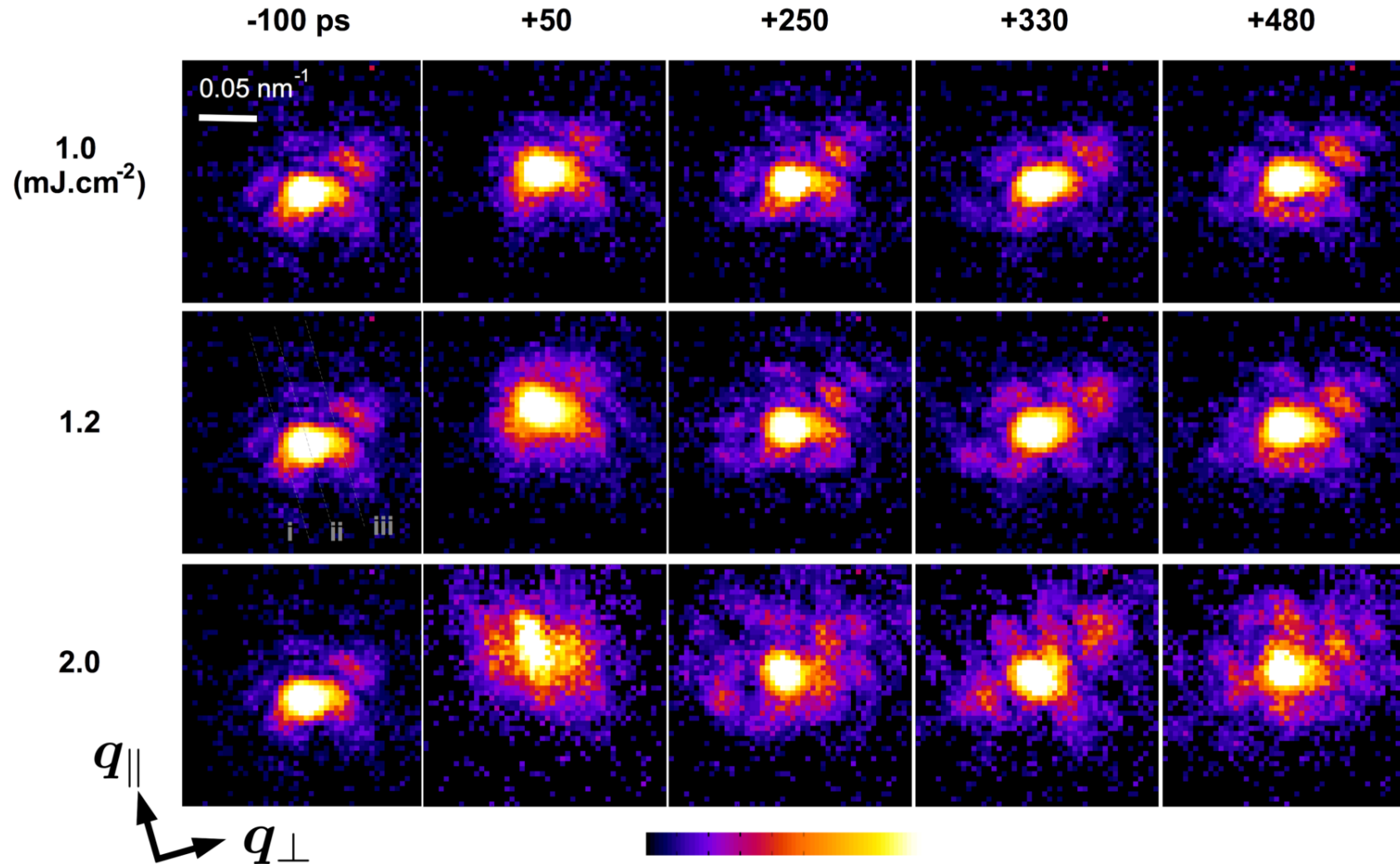
Comparison with (1,1) normal mode of cylinder

Jesse Clark et al, Science 341 56 (2013)



Dependence on Laser Fluence

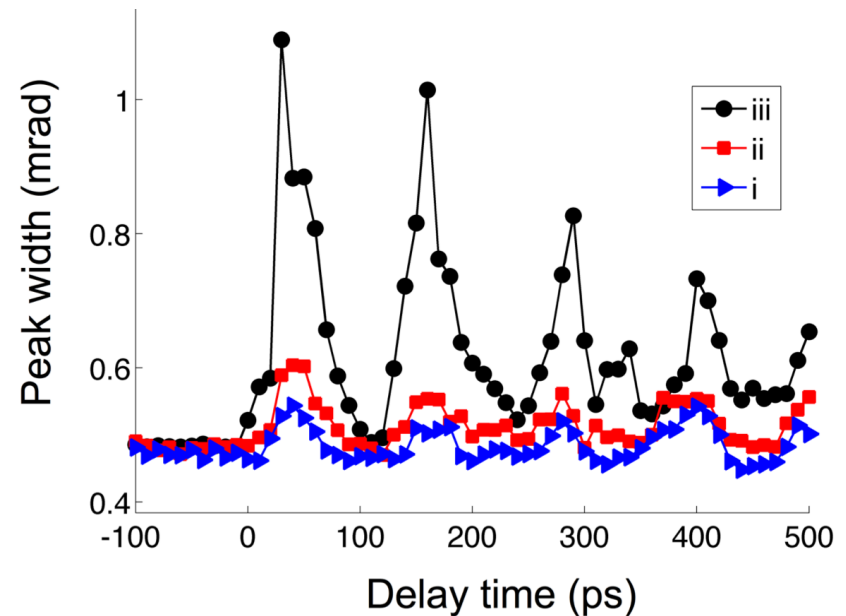
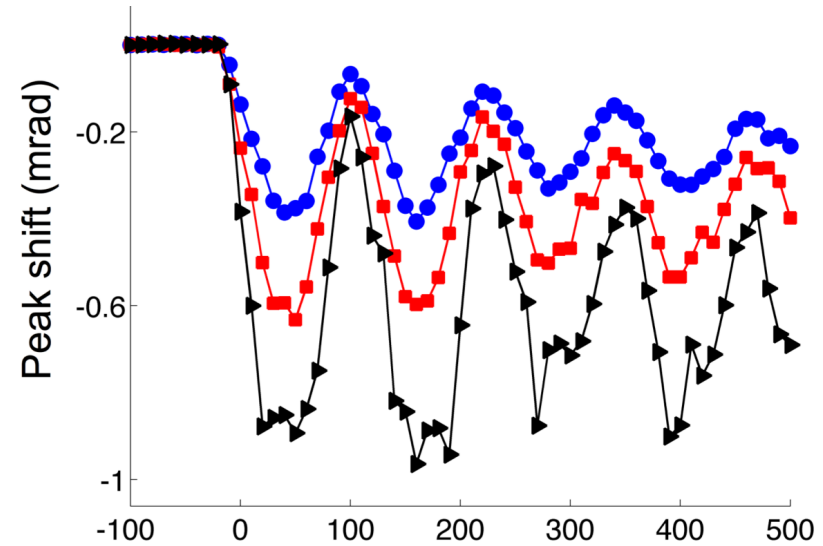
Jesse Clark et al, to be published



Dependence on Laser Fluence

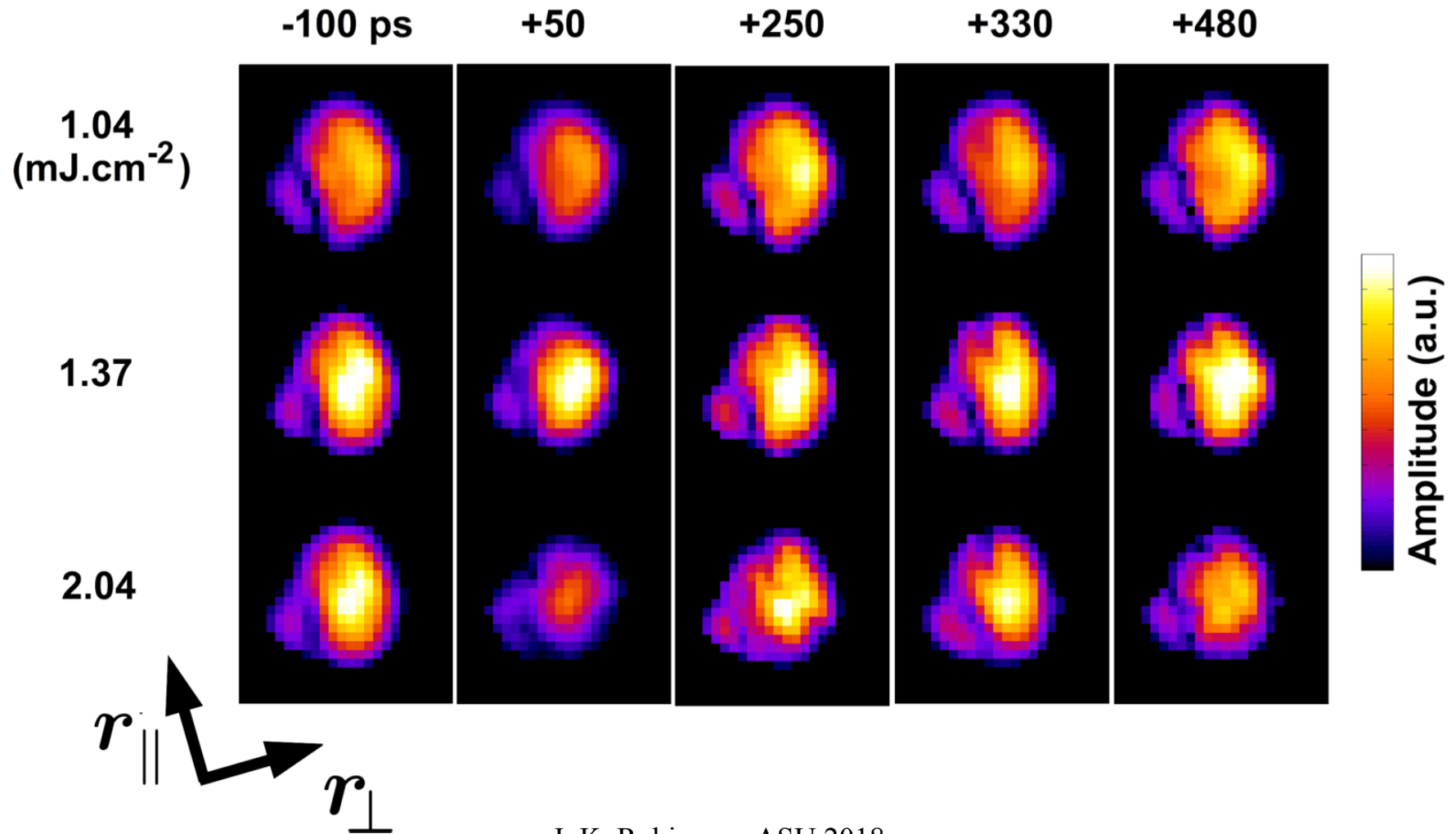
Jesse Clark et al, to be
published

1.0 mJ cm⁻²
1.2 mJ cm⁻²
2.0 mJ cm⁻²

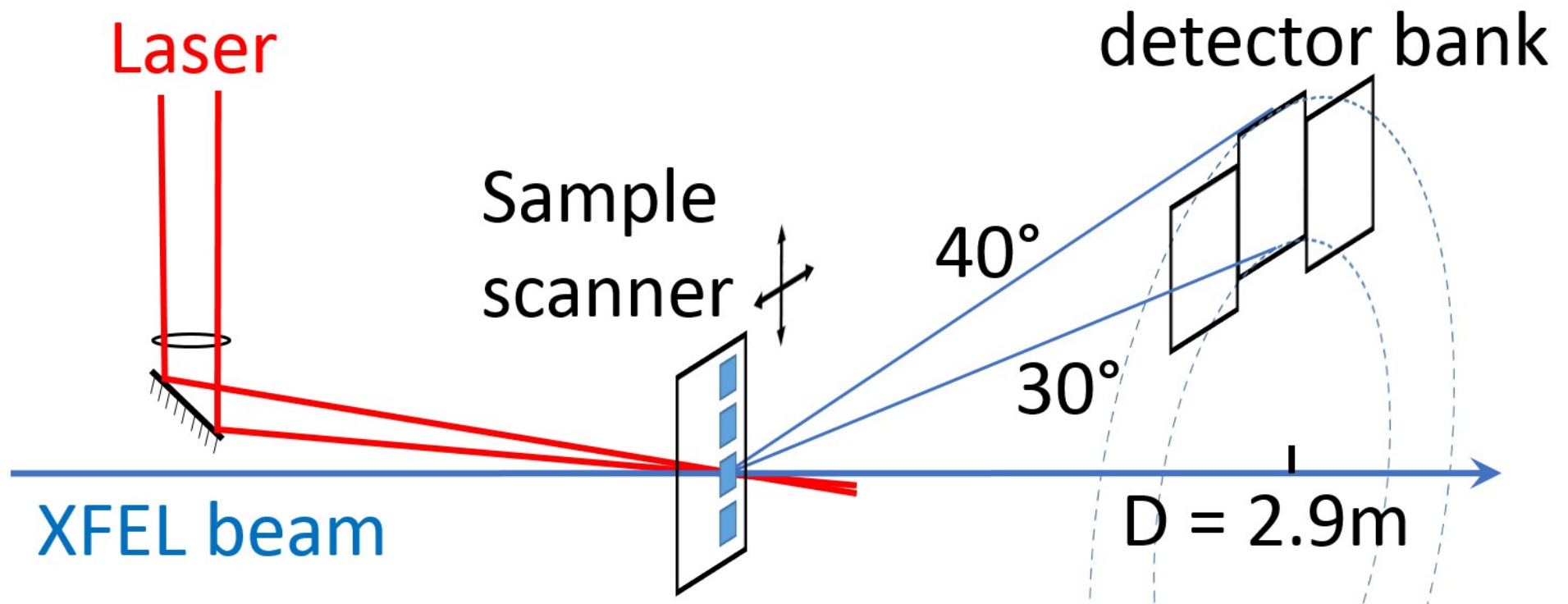


Dependence on Laser Fluence

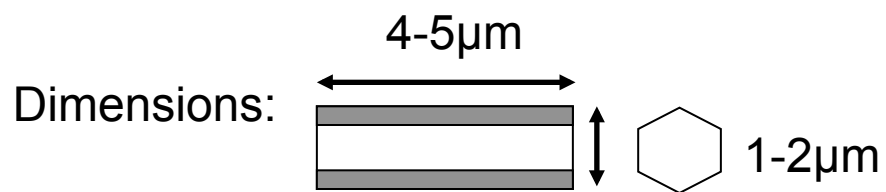
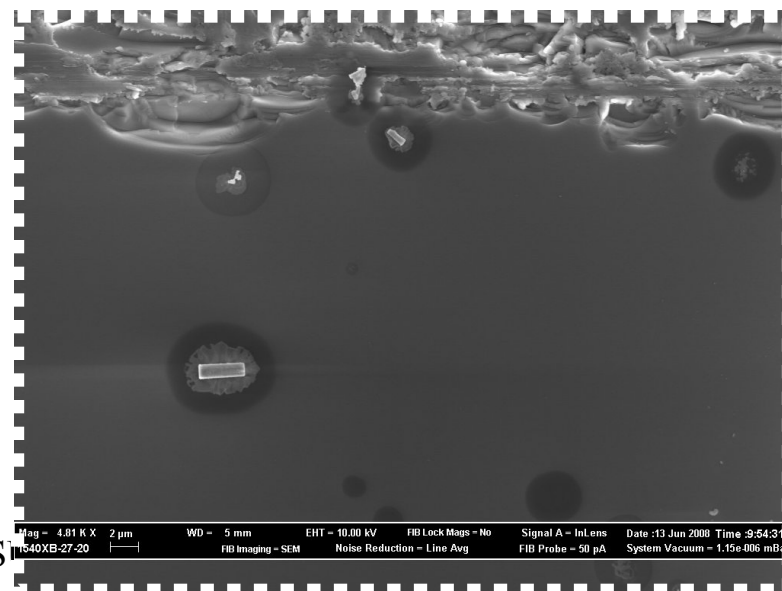
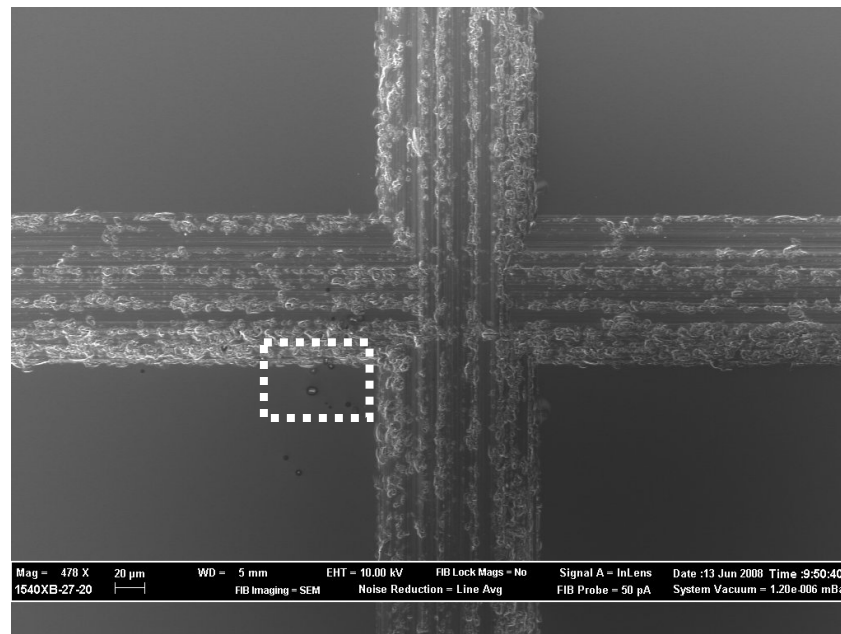
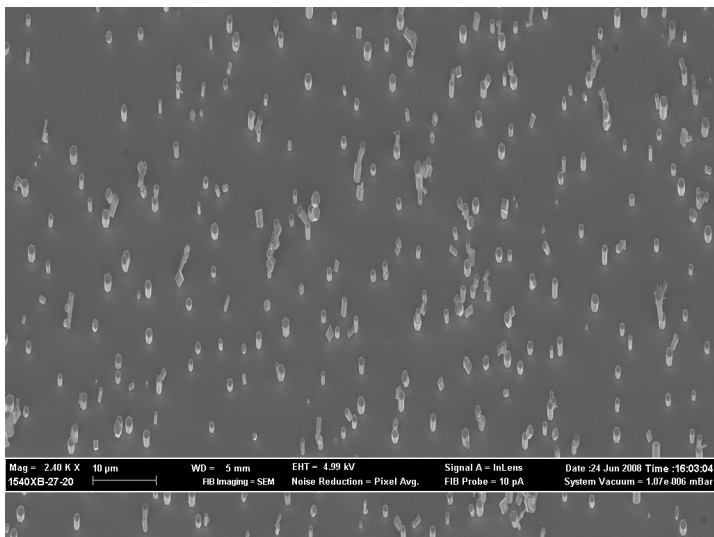
Jesse Clark et al, to be published



Ultrafast Materials Physics Fixed Geometry Setup

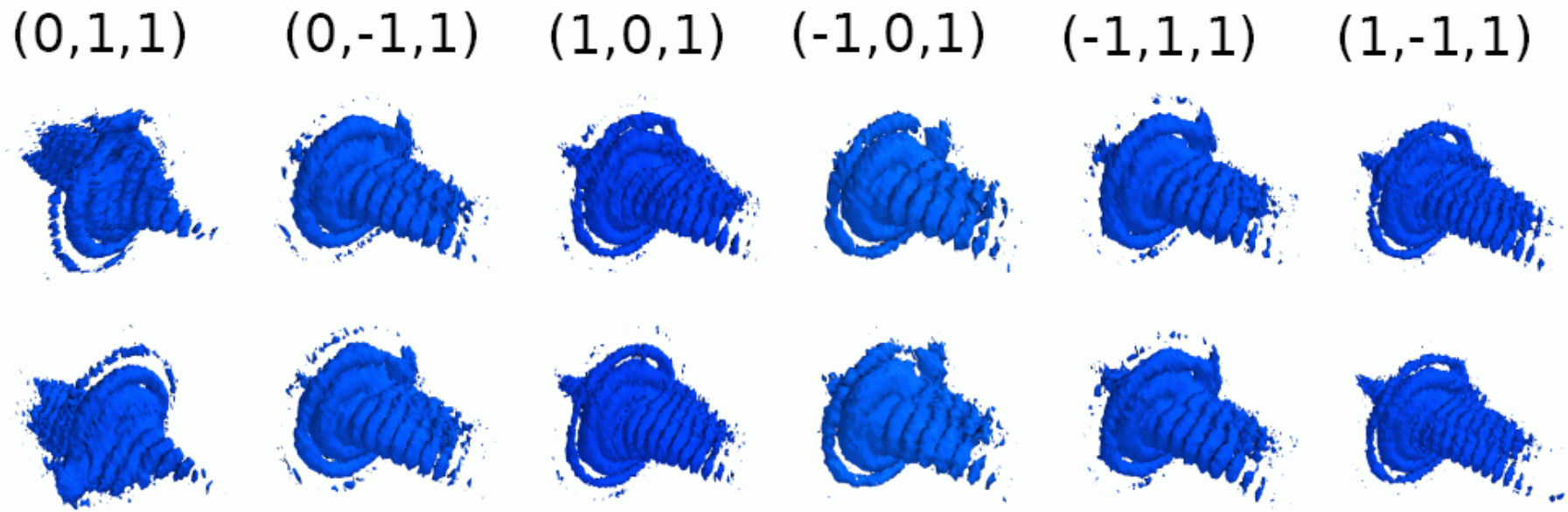


ZnO Sample Preparation



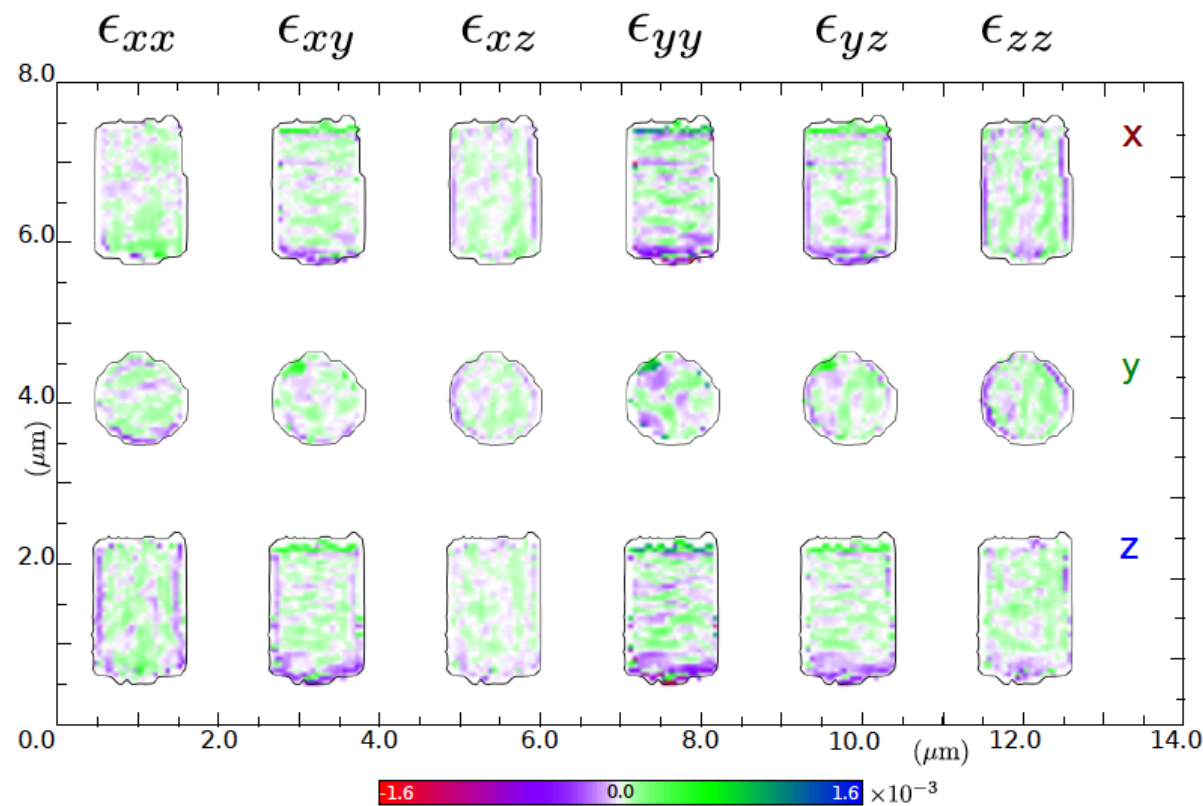
I. K. Robinson, ASU

Extension to 6 Bragg Peaks

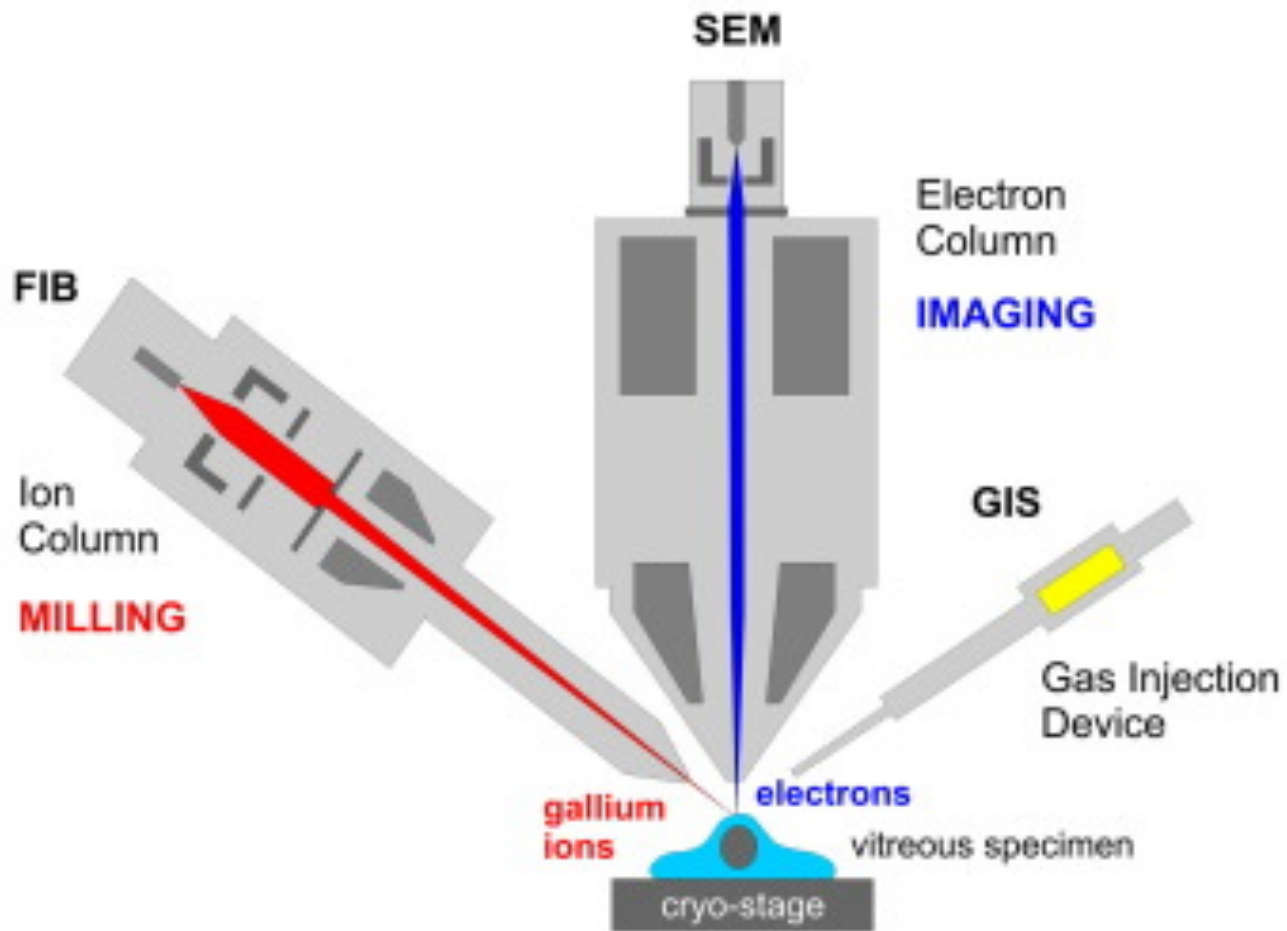


Full Strain Tensor

$$\epsilon_{ij} = \frac{1}{2} \left(\frac{\partial u_j}{\partial x_i} + \frac{\partial u_i}{\partial x_j} \right), \quad \tau_{ij} = \left(\frac{\partial u_j}{\partial x_i} - \frac{\partial u_i}{\partial x_j} \right)$$

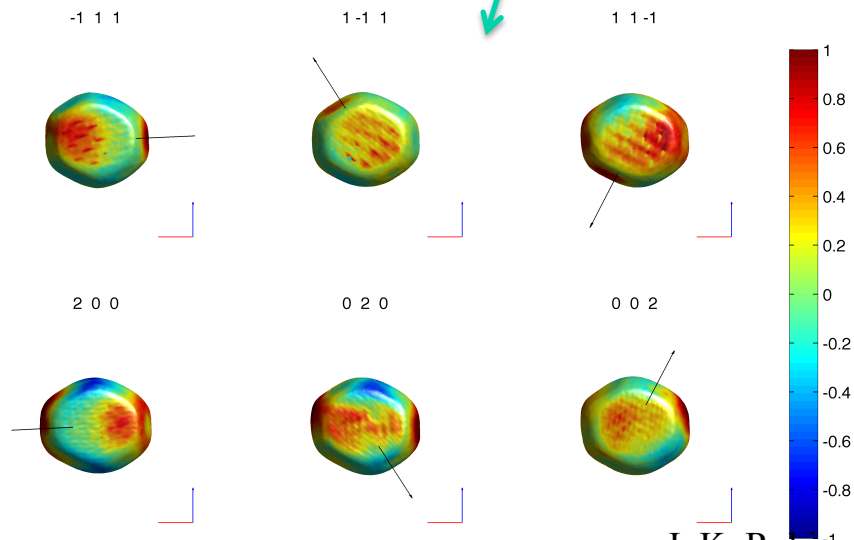
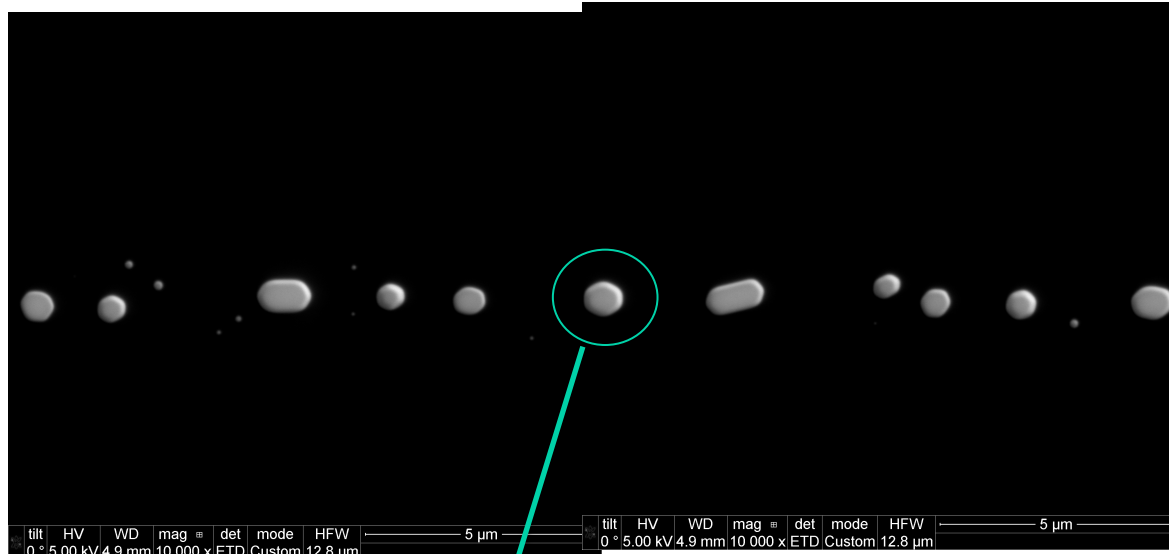


Focused Ion Beam (FIB)



Unimplanted Gold Nanocrystals

Felix Hofmann, Oxford University 34-ID-C



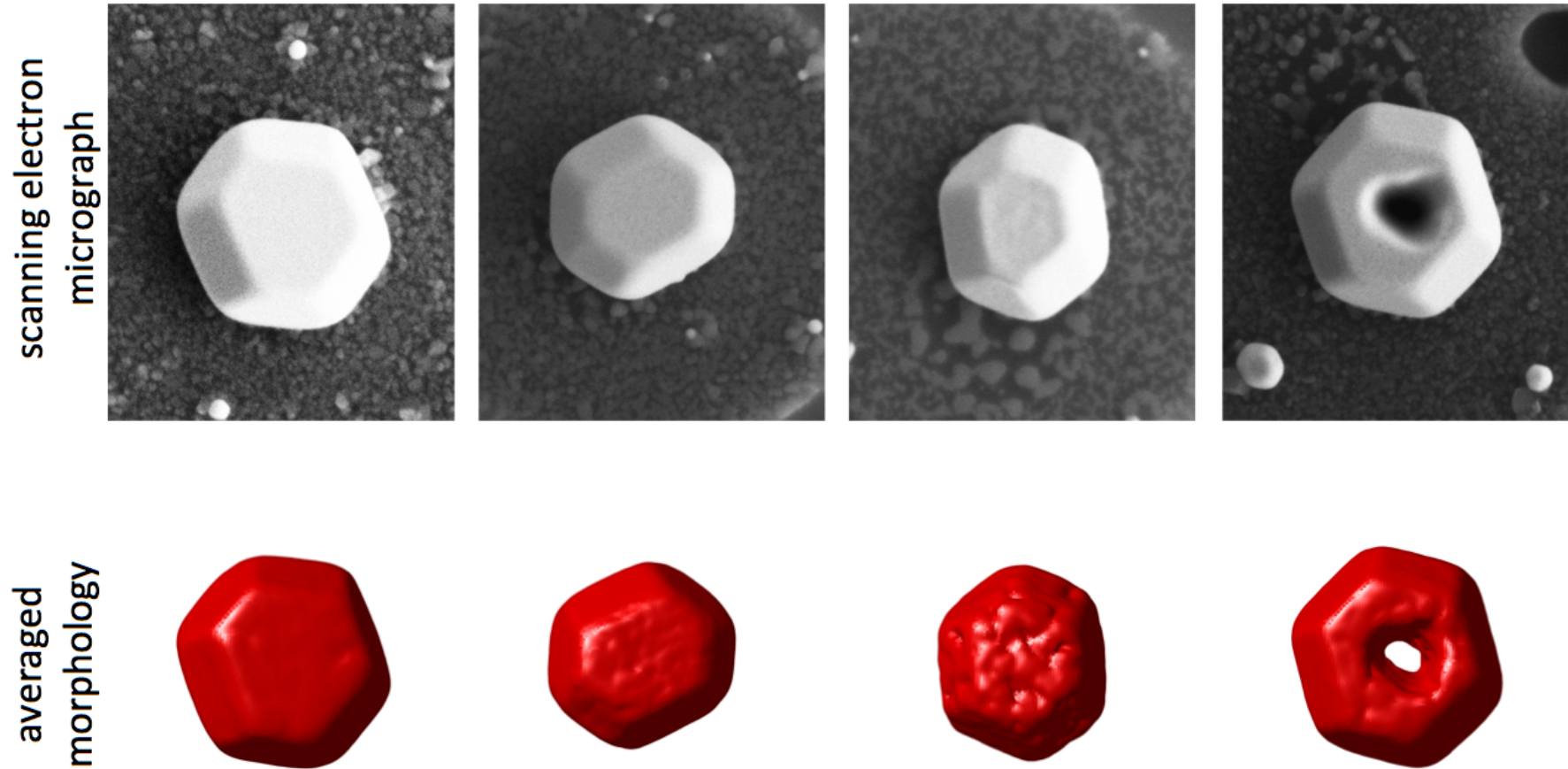
- measured 6 reflections at 9 keV. all phased fine.
- corrected for refraction-induced phase.
- worked out displacement field and hence strains

I. K. Robinson, ASU 2018

phases from different reflections

Shape comparison: BCDI and SEM

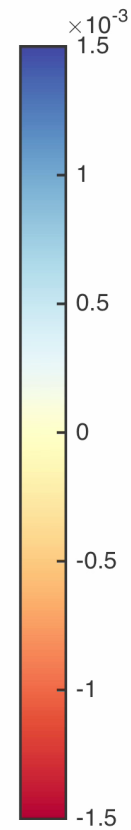
F. Hofmann et al Nature Scientific Reports 7 45993 (2017)



Starting crystal (yz plane)

X position (nm): -430

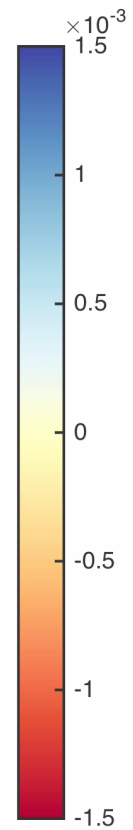
—



After irradiation (yz plane)

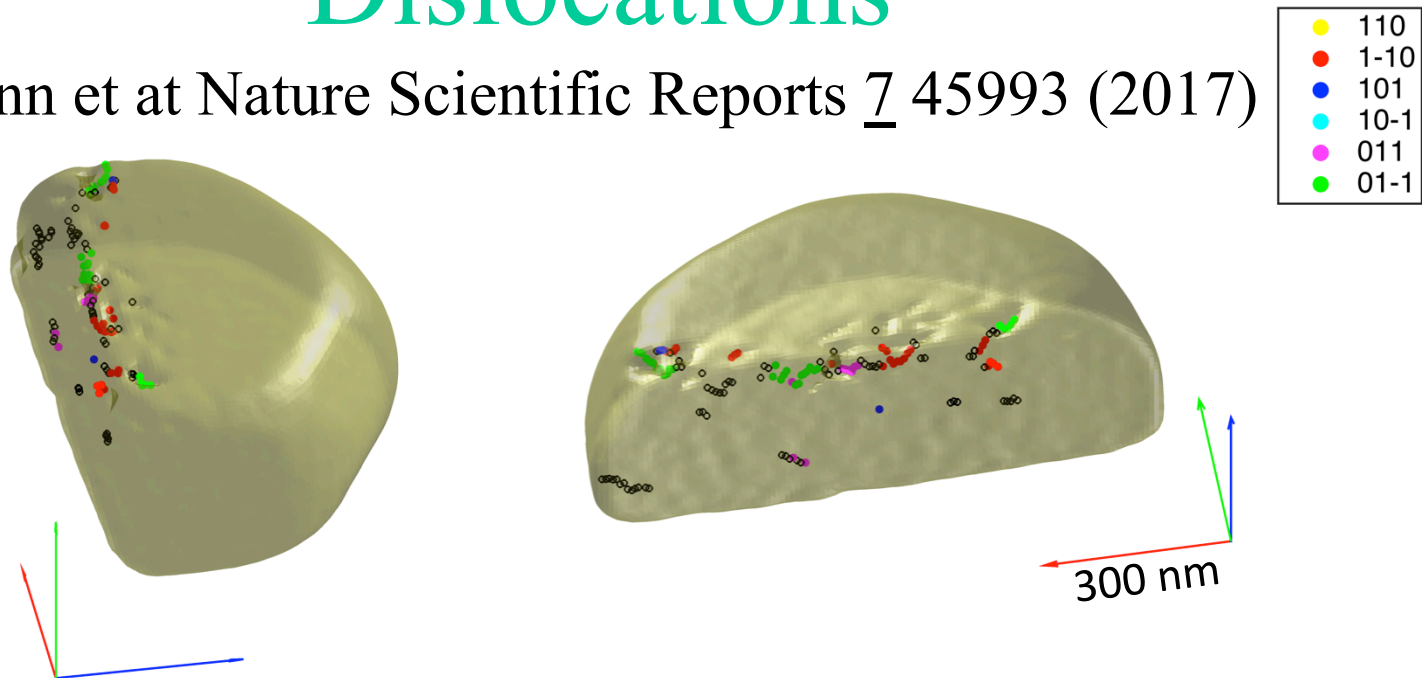
X position (nm): -430

—



Dislocations

F. Hofmann et al Nature Scientific Reports 7 45993 (2017)



Amplitudes and phases of different reflections show jumps and pipes of reduced intensity consistent with dislocations. Dislocations identified in the crystal are shown above. They are colour coded according to their burgers vector direction, determined using Q.b contrast. Dislocations for which the burgers vector direction could not be identified are shown in black.

- dislocations are mostly formed at top edge of crystal where FIB beam has normal incidence component. These can form larger loops.
- some defects can also be seen on the milled face, although these are small.

Bragg Coherent X-ray Diffraction

- Complex density can image strain
- Strain associated with nano-shape
- Diffusion of Cu in Au nanoparticle
- Ultrafast snapshots of vibrations
- Transient melting of nanoparticles
- Strain tensor imaging